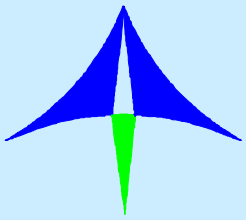

DIRECTORATE OF ENGINEERING AND TECHNICAL EXPLOITATION
NAVIGATION AND SURVEILLANCE DIVISION
ADS PROGRAMME

EUR/SAM RISK ASSESSMENT 2005

DNV-ADS-DOC-337-01/05
DECEMBER 2005

TABLE OF CONTENTS

TABLE OF FIGURES

TABLE OF TABLES

SUMMARY

Two quantitative risk assessments based on suitable verisons of the Reich Collision Risk Model have been carried out for the EUR/SAM Corridor in the South Atlantic, for flight levels between FL290 and FL410. The first assessment concerns the lateral collision risk whilst the second one concerns the vertical collision risk. The vertical collision risk assessment has been split into two parts. The first part consideres the risk due to technical causes, whilst the second one considers the risk due to all causes.

The existing route network, composed of four nearly parallel north-south routes has been analysed, whithout considering traffic on the RANDOM route, placed about 100NM to the west of the current UN-741 and used mainly by IBERIA and LAN-CHILE for northbound traffic. RNP10 and RVSM are implemented within this airspace.

The program CRM in its four-routes version, created by Aena (ADS Programme), has been used to obtain the different parameters of the Reich Collision Risk Model for the current traffic levels. The model outputs for the current situation have been projected over a planning horizon of ten years, assuming traffic growth rates of 4% and 7% per year.

The reliability of the used software was previously assessed comparing the results given by a previous version of the CRM program for three routes with the ones obtained in the collision risk assessment made by ARINC in 2001 ([Ref. 2]). It could be seen that the CRM was conservative in the estimation of the collision risk. Therefore, it was considered to be adequate for this other study, with the required modifications for the four-routes version.

The CRM program uses flight plan data obtained from Picasso, Aena's database, for the Canaries. Some inconsistencies have been detected in this database. Some of these errors have been detected and corrected by software, trying to be conservative. However, some of them may have passed unnoticed. It would be very useful to have flight data from the rest of FIR/UIRs in the EUR/SAM Corridor to be able to cross-check the information obtained from Picasso. These data were not available for this report.

Flight plan data from 22nd January 2005 to 6th November 2005 have been examined to determine the types of aircraft in the airspace, the average flight characteristics of the typical aircraft and the passing frequencies of these aircraft.

The main parameters of the lateral and the vertical collision risk models are the probabilities of lateral and vertical overlap, $P_y(S_y)$[1] and $P_z(S_z)$[2], respectively. Data needed for the computation of lateral and vertical overlap probabilities are the distributions of the lateral and vertical deviations of aircraft from their assigned flight paths. The risk assessments in this report have been hindered considerably by a lack of data on these deviations, particularly on the larger and more infrequent deviations. As a result, conservative assumptions have been made for certain parts of these distributions. In order to confirm the validity of these assumptions and to model the probability distributions accurately, it is recommended that additional data collections be reported from appropiate monitoring procedures.

The probability density of the lateral deviations has been modelled as a double double exponential distribution. This approach was also used by ARINC in the aforementioned study. This distribution is divided into a core part, whose parameter was derived from the RNP type, i.e. RNP10 and the tail part, where atypical errors are taken into account.
The value of the lateral overlap probability decreases as the lateral separation between routes increases, being the estimated value for the minimum separation, 50NM, $P_y(50) = 8.645 \times 10^{-5}$.

The probability of vertical overlap due to technical causes was based on the probability distribution of Total Vertical Error (TVE). This was obtained by convoluting probability distributions of Altimetry System Errors (ASE) and typical Assigned Altitude Deviation

[1] $P_y(S_y)$ is the probability of lateral overlap of aircraft nominally flying on laterally adjacent paths at the same flight level.

[2] $P_z(S_z)$ is the probability of vertical overlap of aircraft nominally flying on adjacent flight levels of the same track.

(AAD). In the absence of any direct monitoring data from the EUR/SAM Corridor, height-keeping data and models from the EUR airspace have been used. These data were also being reviewed when this assessment was made. So, it would be recommended to repeat this study when definitive data from the EUR report are available.

The value of the vertical overlap probability obtained for S_z=1000ft is $P_z(1000) = 1.5447 \times 10^{-9}$. A more conservative value, used in the NAT has also been considered, i.e. $P_z(1000) = 2.46 \times 10^{-8}$.

The next important parameters of the two collision risk models are the lateral and vertical occupancies, E_x[3] and E_z[4]. These are measures of the exposure to the loss of lateral and vertical separation in relation to the amount of traffic in the airspace. Occupancies for current traffic levels have been calculated by the CRM program.

Occupancy due to crossing traffic is also needed for the vertical risk assessment. These data were not available. Therefore, the values obtained by ARINC in [Ref. 2] have been projected to the current time using the appropriate traffic growth factor.

The rest of the parameters of the collision risk models, such as average speed, average relative velocities or aircraft dimensions have also been given by the CRM software.

With all these parameters, the lateral and the technical vertical risk have been assessed and they have been compared with the maximum value allowed, $TLS = 5 \times 10^{-9}$ and $\mathrm{TLS} = 2.5 \times 10^{-9}$, respectively. Nevertheless, it has not been possible to estimate the overall

[3] E_y is the lateral occupancy, i.e, the average number of aircraft flying on laterally adjacent tracks at the same flight level within segments of length $2S_x$ centered on the typical aircraft.

[4] E_z is the vertical occupancy, i.e, the average number of aircraft flying on adjacent flight levels of the same track within segments of length $2S_x$ centered on the typical aircraft.

vertical risk due to lack of large height deviation reports. This value should be less than $TLS = 5 \times 10^{-9}$.

For current traffic levels, the lateral collision risk obtained is 1.62×10^{-9}, whilst the lateral collision risk estimated for 2015 with an annual traffic growtht rate of 4% is 2.40×10^{-9} and 3.19×10^{-9} if the annual traffic growth rate is of 7%. These values don't take into account traffic on the RANDOM route. Nevertheless, since traffic on this route only represents 5% of the traffic in the Corridor, it is considered that the collision risk due to this route will not make the collision risk go above the TLS and the system is considered to be laterally safe until 2015.

As far as the technical vertical risk is concerned, the value of the collision risk for the current traffic levels is estimated to be 8.01×10^{-11} or 1.28×10^{-9}, depending on the vertical overlap probability used (the first value corresponds to the calculated $P_z(1000)$ and the second one, to the conservative value used in the NAT). The technical vertical collision risk estimated for 2015 with an annual traffic growth rate of 4% is 1.19×10^{-10} for the calculated vertical overlap probability and 1.89×10^{-9} for the NAT probability. If the annual traffic growth rate is of 7% the technical risk is 1.58×10^{-10} and 2.51×10^{-9}, depending again on the vertical overlap probability used.

It can be seen that the values are under the TLS for technical vertical risk, 2.5×10^{-9}, even in 2015 and with an extremely conservative vertical overlap probability.

As it has been said, it has not been possible to obtain the overall vertical risk, since no large height deviation reports were available from the EUR/SAM Corridor.

1.- INTRODUCTION

This report assesses the current and projected lateral and vertical collision risk in the EUR/SAM Corridor between FL290 and FL410, where RNP10 and RVSM are implemented.

For this study, the program CRM, in its four-routes version, has been used. It is a program created by Aena for collision risk analysis, based on the Reich Collision Risk Model.

The values given by the CRM correspond to the time period analysed, 2005 in this case. Taking these values into account and the traffic forecast for the future, it is possible to estimate the collision risk for the following years.

2.- AIRSPACE DESCRIPTION

As it has already been said, the airspace analysed in this report is the EUR/SAM Corridor, which lies in the South Atlantic airspace between the Canary Islands and Brazil.

Figure 1 shows the existing route network together with the horizontal boundaries of the area to be considered in the risk assessment.

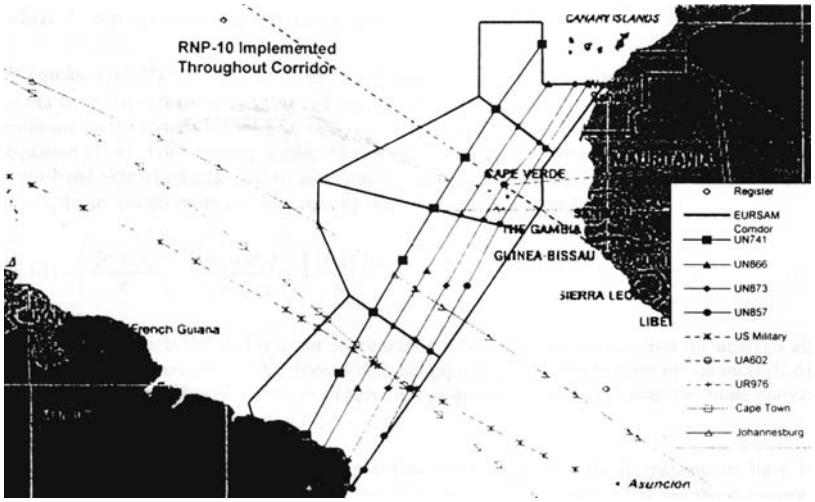

Figure 1
Existing route network

The existing route network is composed of four nearly parallel north-south routes situated within the Canaries UIR, SAL Oceanic UIR/UTA, Dakar Oceanic UIR and Recife FIR.

The denomination of the routes is, from west to east, UN-741, UN-866, UN-873 and UN-857, and their magnetic direction varies around 45º for northbound traffic and 225º for southbound traffic.

Minimum lateral separation between routes is 110NM for routes UN-741/UN-866, 90NM for routes UN-866/UN-873 and 50NM for routes UN-873/UN-857.

RNP10 and RVSM are implemented within this airspace.

There is northbound traffic and southbound traffic in all the routes and the flight level allocation scheme in use from 20th January 2005 is the following:

- Southbound flight levels: FL300, FL320, FL340, FL360, FL380 and FL400.
- Northbound flight levels: FL290, FL310, FL330, FL350, FL370, FL390 and FL410.

The following figure shows a detailed image of the tracks system, with all the fixes or Waypoint Position Reporting Points that define them:

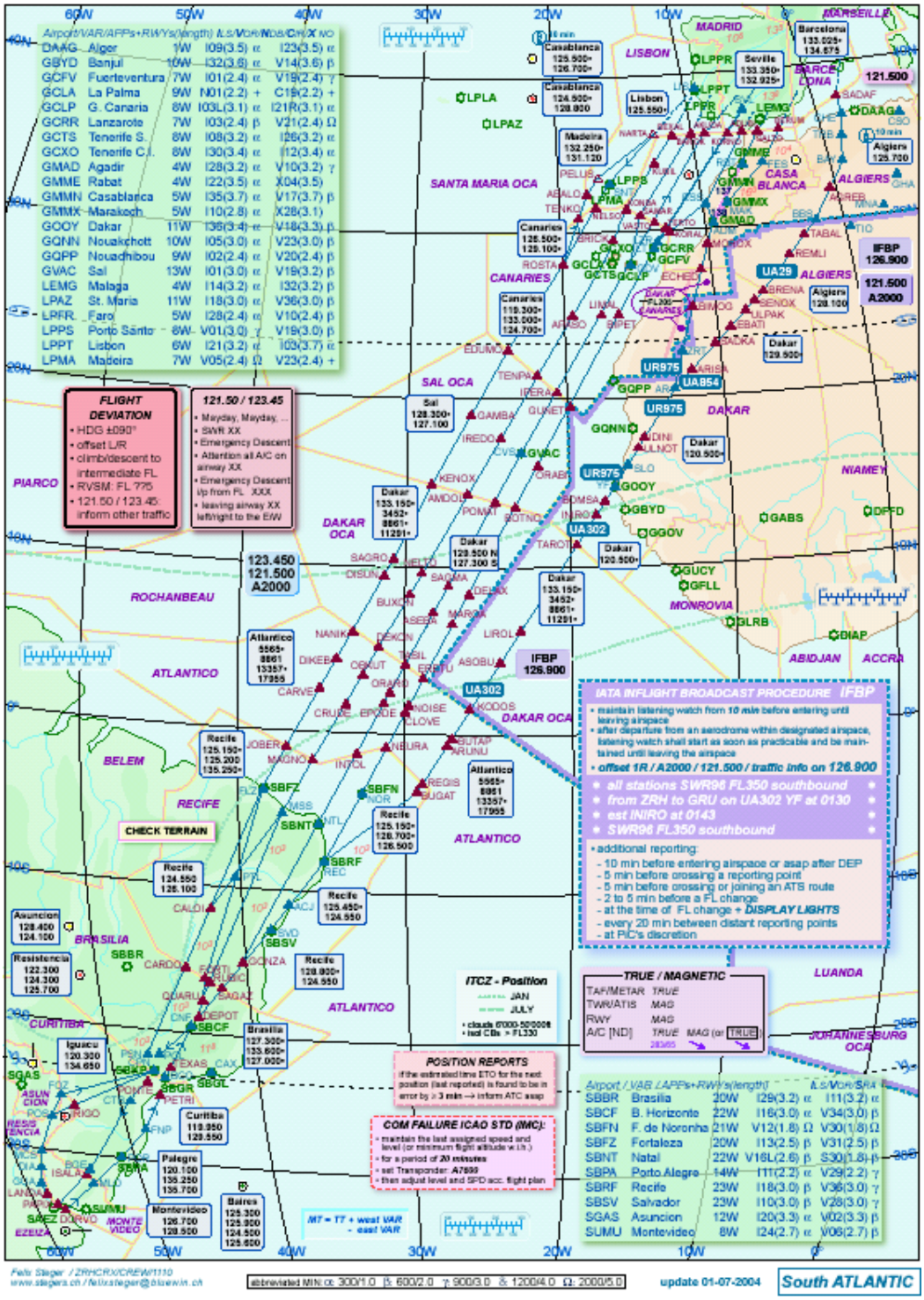

Figure 2
EUR/SAM Corridor

An enlarged image of the routes system and a scheme in the Canaries UIR, section in which the study has been made, are shown in Figure 3 and in Figure 4, respectively.

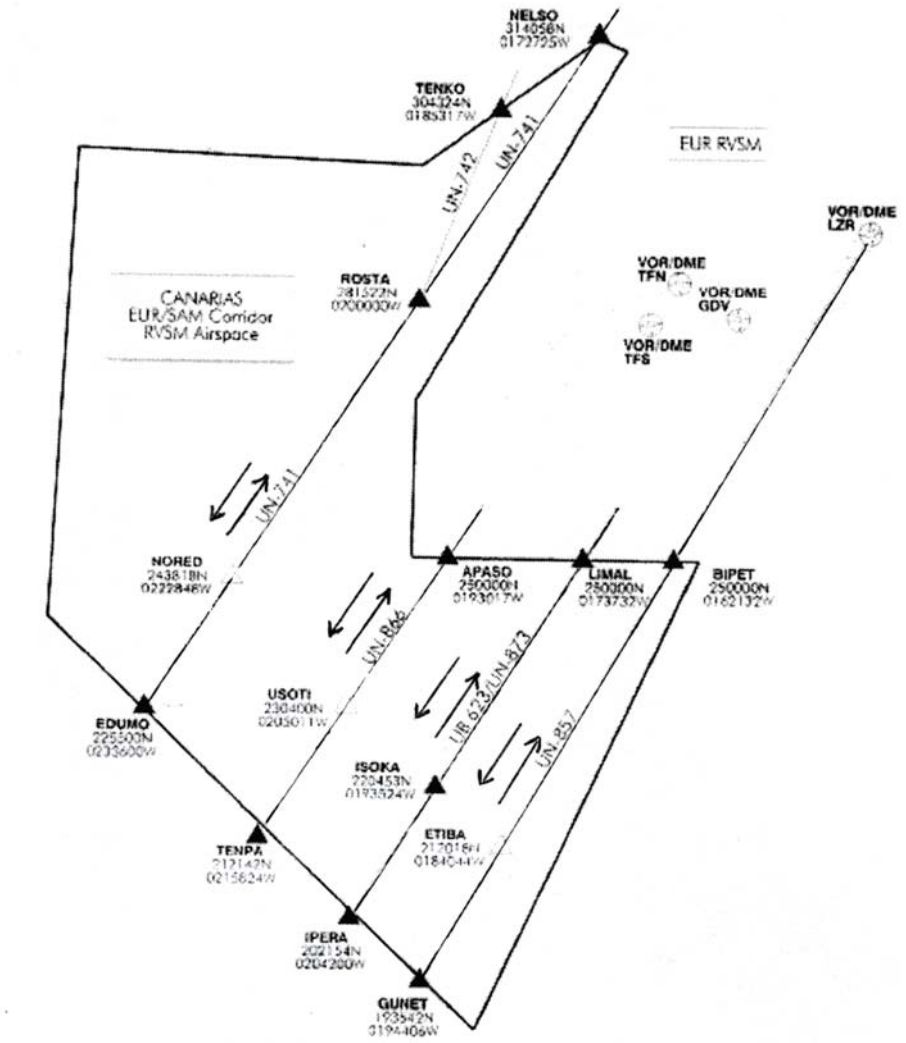

Figure 3
EUR/SAM Corridor in Canaries UIR airspace

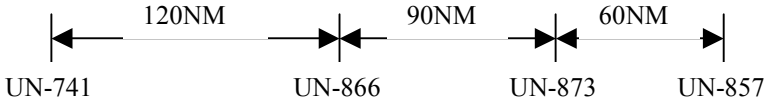

Figure 4
Current routes system

Besides these four routes, there is an additional route, called RANDOM, placed about 100NM to the west of the current UN-741, used mainly by IBERIA and LAN-CHILE for northbound traffic.

These aircraft cross the following points:

- 25 00 03N, 24 59 59W
- 30 00 01N, 20 59 59W

Southbound traffic of these airlines has also been detected in the route defined by:

- Nelso
- Rosta
- 24 59 57N, 23 00 02W
- 23 26 58N, 24 19 03W

Although the number of aircraft on these routes will be indicated later, they have not been considered in the collision risk assessment.

Apart from these routes, Figure 1 shows that there is some traffic crossing the Corridor in the SAL UIR, in the Dakar UIR and in the Recife FIR.

2.1.- ATS SERVICES AND PROCEDURES

The airspace in the area of the South Atlantic EUR/SAM Corridor is subject to procedural control with pilot voice waypoint position reporting. While VHF voice communications are available over approximately the same areas where DME coverage is available, the primary means of communications is HF voice. Appropriately equipped aircraft can also use SATCOM and HF Data Link (HFDL) throughout the South Atlantic EUR/SAM Corridor.

There are two DME stations inside the RNP10 airspace, namely CVS, Almilcar Cabral, and NOR, Noronha. Their ranges are limited by the RF horizon to about 200NM.

There are also some DME stations to the north and south of the RNP10 airspace, in the Canary Islands and in Recife.

Although radar surveillance is not available for the parallel route system in the four FIR/UIRs, it is available in the adjacent canaries TMA, on the coast of Brazil and Cape Verde. Radar range is also limited by de RF horizon.

These radars do provide an opportunity to monitor the lateral and the vertical deviations of aircraft flying in the Corridor. However, information from these radars was not available for this study.

The system called SACCAN (ADS-CPDLC in the Canaries Fir) is also installed in the Canary Islands. The main purpose of SACCAN, after proper technical and operational evaluation and valiation, is to provide air traffic control services to FANS 1/A aircraft operating in the Canary airspace.

FANS 1/A equipped aircraft use the SITA and ARINC networks and can communicate with SACCAN by means of the Aeronautical Mobile Satellite Service (AMSS) provided by INMARSAT, or by VHF when within the range of any of the multiple SITA or ARINC VHF data link stations, like the two of SITA located in the Canary Islands.

The technical coverage of SACCAN is the coverage provided by the constellation of geostationary satellites INMARSAT, i.e. global coverage (except for the poles). Nevertheless, operationally, the area of interest is the oceanic area of the Canaries FIR where there is not radar coverage.

SACCAN uses FANS-1/A technology. The system improves surveillance (with ADS) and communications (with CPDLC) of the FANS-1 or FANS-A equipped aircraft, when flying over the oceanic area of the Canaries FIR.
The system has made possible to realize two operational evaluation phases.

This study does not condider the reduction of the collision risk that would be obtained with the use of ADS.

2.2.- DATA SOURCES AND SOFTWARE

The starting point of this study is the flight progress data stored in Picasso, Aena's database, for the Canaries. It consists of initial flight plan data updated by the controllers with pilot position reports.

Occasionally, it can happen that due to workload constraints controllers, although obviously updating their personal flight progress information, do not enter the information into the database system. As a consequence, the altitude information obtained from Picasso is not always correct. In the same way, it is possible that typographical errors have been introduced while inputting the information or that some of this information has been omitted. Some of these errors have been detected and corrected by software, as it will be explained later on.

The analysed flight plans are those which include the waypoints ROSTA and EDUMO, APASO and TENPA, LIMAL and IPERA and BIPET and GUNET, that define routes UN-741, UN-866, UN-873 and UN-857 respectively, covering the time period 22nd January 2005 to 6th November 2005.

Although traffic in the RANDOM route has been studied in order to know how many aircraft fly on this route, these aircraft have not been considered in the calculation of collision risk.

The study is limited to flights between FL290 and FL410.

Data obtained from flight plan data and needed for the study are: aircraft type, flight level and date and time of waypoint crossing.

No information from the rest of FIRs/UIRs was available for this study. This information would have been useful to crosscheck data from the Canaries database.

In the collision risk assessment made by ARINC ([Ref. 2] in 2001, that was the base for RNP10 implementation in the South Atlantic Corridor and for the introduction of the current route UN-873, it was mentioned that several errors regarding flight level were identified in the flight plans because a high proportion of flights did not match the vertical route structure.
This has been verified analysing some flight plans from Picasso, chosen by chance.
The used software takes this into account and corrects altitudes assuming that:

- All aircraft conform to the vertical route structure
- No aircraft entered or left the vertical route structure.
- The reported altitudes are close to the actual altitudes.
- The reported altitudes are less than the actual altitudes.

2.2.1.- Software

For this study the program CRM, in its four-routes version, has been used. It is a program created by Aena for collision risk analysis.

The theoretical foundation of this program is the Reich Collision Risk Model.
It searches in Picasso database for the data needed and calculates the different parameters that appear in lateral and vertical collision risk and the risk value.

The values given by the CRM correspond to the time period analysed, 2005 in this case. Taking these values into account and the traffic forecast for the future, it is possible to estimate the collision risk for the following years.

As it will be explained hereinafter, the calculation of this estimate is very simple and it is not done by the CRM, but with Excel sheets.

Before this four-routes version, the CRM program for three routes was created in order to verify its reliability, comparing the results given by the program with the ones obtained by ARINC in the study previously mentioned ([Ref. 2]).
After this comparison, detailed in [Ref. 3], it could be seen that results were similar in both cases, being the collision risk slightly bigger with the CRM program. So, it was considered to be conservative and adequate for this other study, with the required modifications that led to the four-routes version.

As it has already been said, the program corrects the errors that have been detected in the Picasso database.

2.3.- AIRCRAFT POPULATION

The most common aircraft types, the number of flights per type and the proportion of these types over the total of flights detected during the time period considered between FL290 and FL410 have been analysed from the Canaries flight information database.
Table 1 shows these values together with the geometric dimensions of these aircraft types.

Aircraft type	Count	% AC	Length (m)	Wingspan (m)	Height (m)
B777-200	3109	15.27	63.70	60.90	18.50
A340-300	2727	13.40	63.70	60.30	16.74
MD11	2260	11.10	61.20	51.70	17.60
B767-300	2036	10.00	47.60	54.90	15.90
A310	1991	9.78	46.40	43.89	15.80
B747-400	1853	9.10	70.70	64.40	19.40
A330-200	1367	6.72	63.70	60.03	16.74
A340-600	1178	5.79	74.37	63.60	17.80
B757-200	1078	5.30	47.32	38.05	13.60
B747-200	685	3.37	70.70	59.60	19.30
A320-100	363	1.78	37.57	34.10	11.76
A320	311	1.53	46.66	43.90	15.80
A330-300	227	1.12	63.70	60.03	16.74
A340-200	217	1.07	59.39	60.30	16.74
B737-800	196	0.96	39.47	34.31	12.50
DC10	102	0.50	55.20	50.40	17.90
B777-300	66	0.32	73.90	60.90	19.30
F900	63	0.31	20.20	19.30	7.60
A340	46	0.23	59.39	60.30	16.70
L101	39	0.19	50.05	50.09	16.80
A319	33	0.16	33.84	34.10	11.76
E135	29	0.14	26.33	20.04	6.76
B737	28	0.14	33.60	34.30	12.50
B747-300	26	0.13	70.66	59.64	19.33
GLF4	25	0.12	26.90	23.79	7.64
B707-300	25	0.12	46.60	44.42	12.93
CL60	24	0.12	20.86	19.35	6.28
F2TH	21	0.10	20.21	19.33	7.55
H25B	16	0.08	15.60	15.70	5.40
B757-300	16	0.08	54.47	38.05	13.56
FA50	15	0.07	18.52	18.96	6.97
E170	14	0.07	29.90	26	9.67
B737-200	14	0.07	30.54	28.34	11.28
LJ35	13	0.06	14.71	11.97	3.71
B737-500	13	0.06	31.01	28.90	11.10
GLEX	12	0.06	30.30	28.65	7.57
C750	10	0.05	22.05	19.38	5.84
GLF5	8	0.04	29.42	28.50	7.87
Otros	100	0.49	---	---	---

Table 1
Aircraft population and number of flights per type

The data sample includes 20359 flights of 78 different aircraft types. The population is dominated by large airframes such as B777-200, A340-300, MD11, B767-300, A310 and B747-400. These six types make up about 68.65% of the total number of flights.
The next 9 types, that also belong to the Airbus and Boeing families, make up another 27.64% and the rest, 3.71% is distributed among the other 63 aircraft types.

2.4.- TEMPORAL DISTRIBUTION OF FLIGHTS

Figure 5 shows the distribution of the number of flights per day in EDUMO, TENPA, IPERA and GUNET from 22nd January 2005 to 6th November 2005, differentiating between Northbound (NB) and Southbound (SB) traffic.

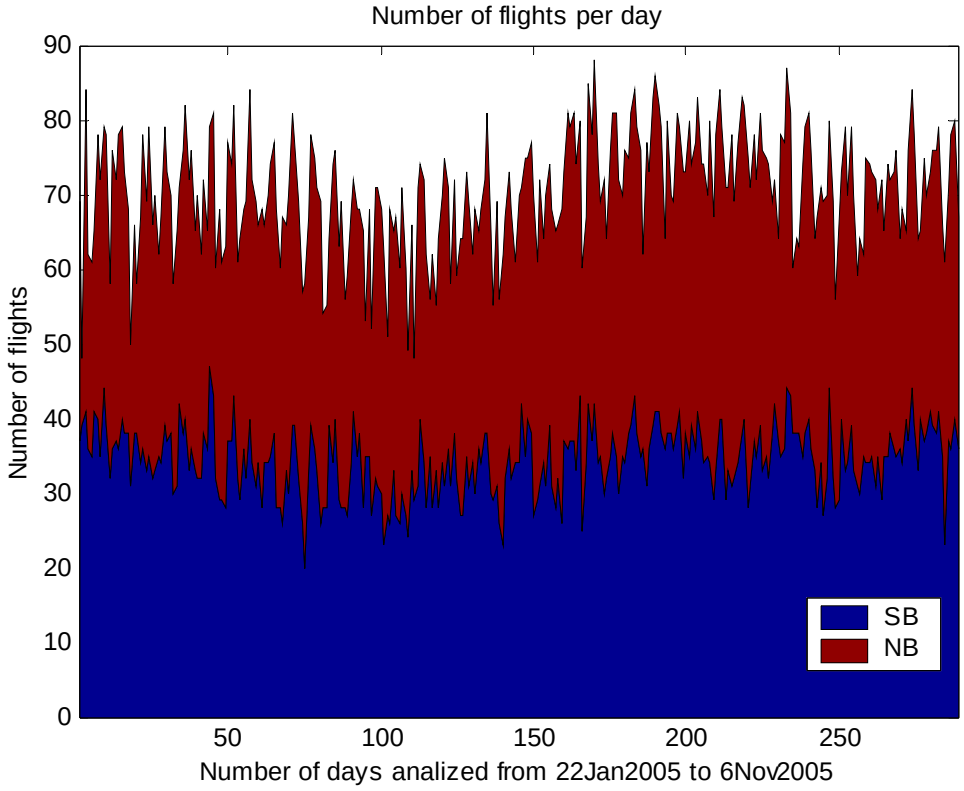

Figure 5
Number of flights per day

The overall average traffic is 70.4 flights per day with a standard deviation of 7.73 flights per day.

Figure 6 shows the distribution of the same traffic over the days of the week.

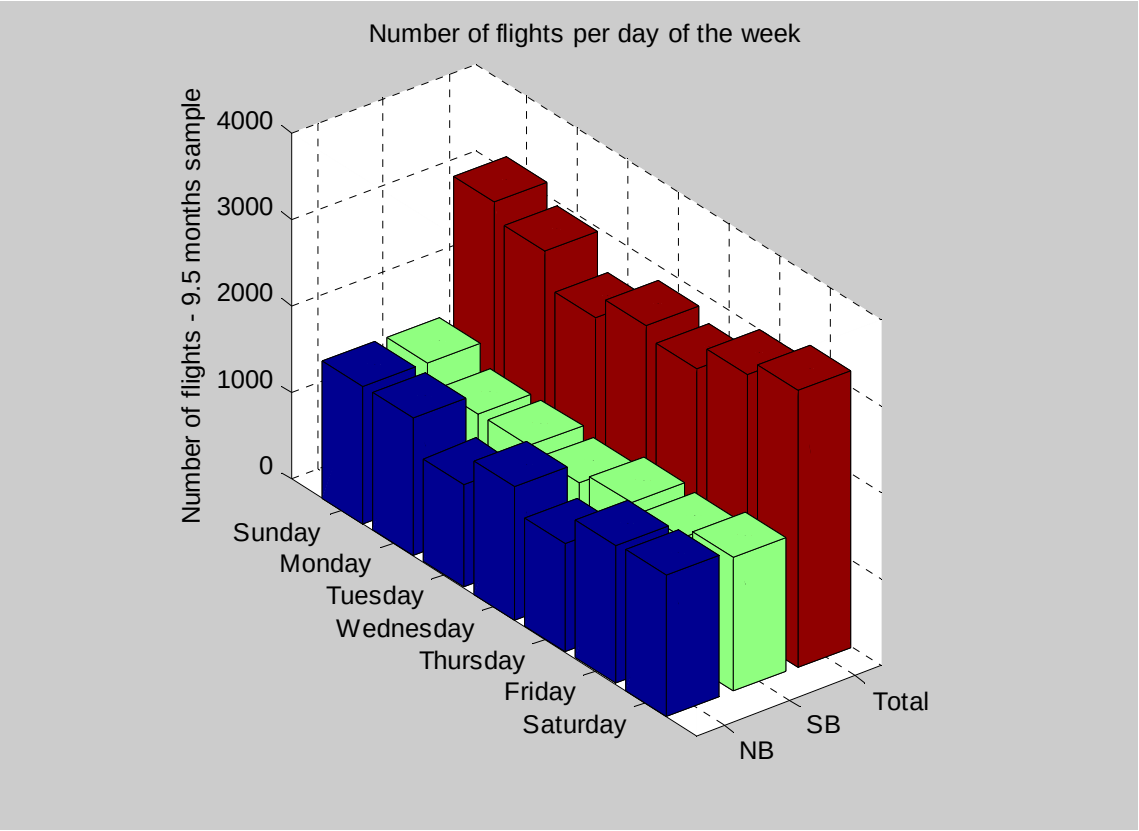

Figure 6
Number of flights per day of the week

In the following two figures what is shown is the distribution of flights per hour.
The first one shows the distribution of flights obtained with the time of waypoint crossing in EDUMO, TENPA, IPERA and GUNET, distributing the 20359 aircraft detected over the studied period according to the time of day at which they crossed those waypoints.
It also distinguish between Northbound (NB) and Southbound (SB) traffic.

It can be seen that from 00:00h to 3:00h and, in a lower extent, from 13:00h to 20:00h is when the highest concentration of southbound flights occur, whilst most of the northbound aircraft concentrate between 00:00h and 10:00h.

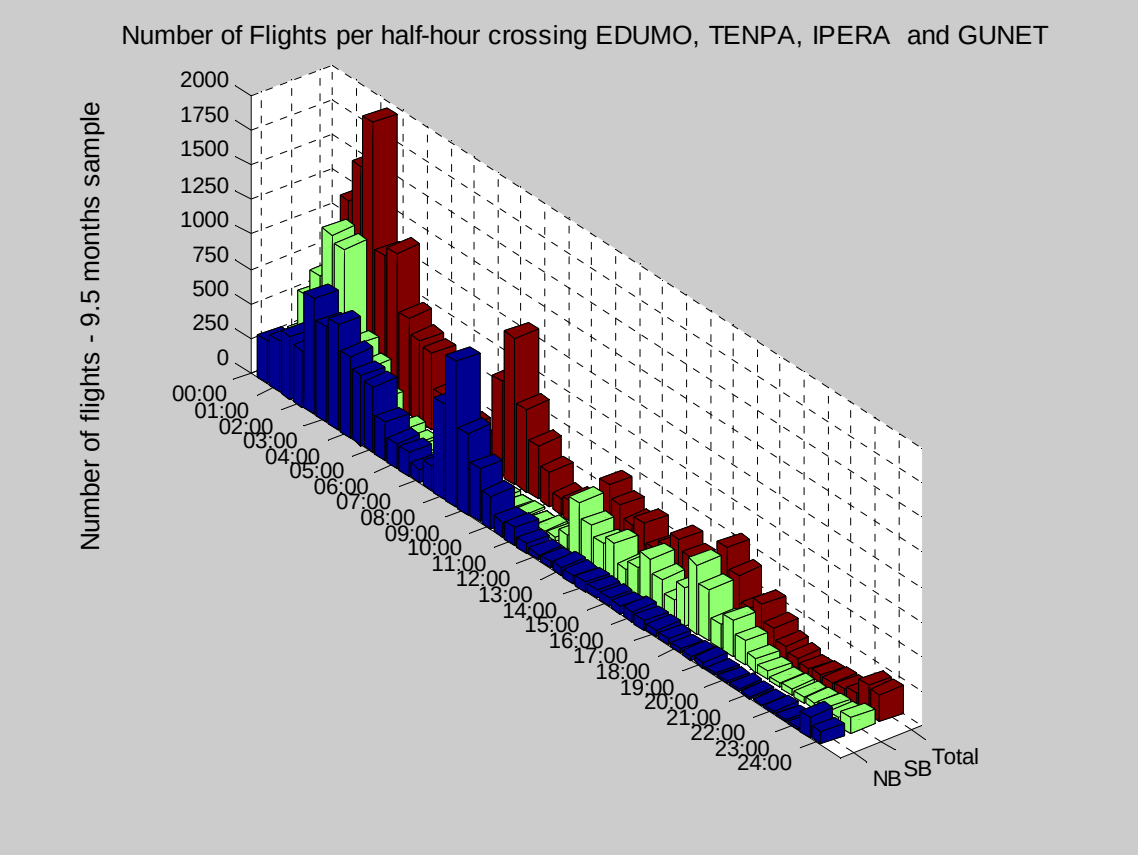

Figure 7
Number of flights per hour crossing EDUMO, TENPA, IPERA and GUNET

The traffic distribution at any other point in the route system can be extrapolated from the distributions measured at any one plane. This is accomplished by moving the north and southbound distributions measured at one plane along the time axis in opposite directions and multiplying this time shift by the average aircraft speed.

So, if the southbound distribution obtained in Figure 7 is shifted 3.5 hours forward in time and the northbound distribution is shifted 3.5 hours back in time, and an average speed of 480kts is considered, the distribution shown in Figure 8 is obtained, which represents the distribution about 1680 NM to the south. That corresponds to Recife FIR.

In this figure it can be seen that the highest traffic concentration in the route system occurs in the southern most segment of the route system, under Recife control, between 4:00h and 7:00h.

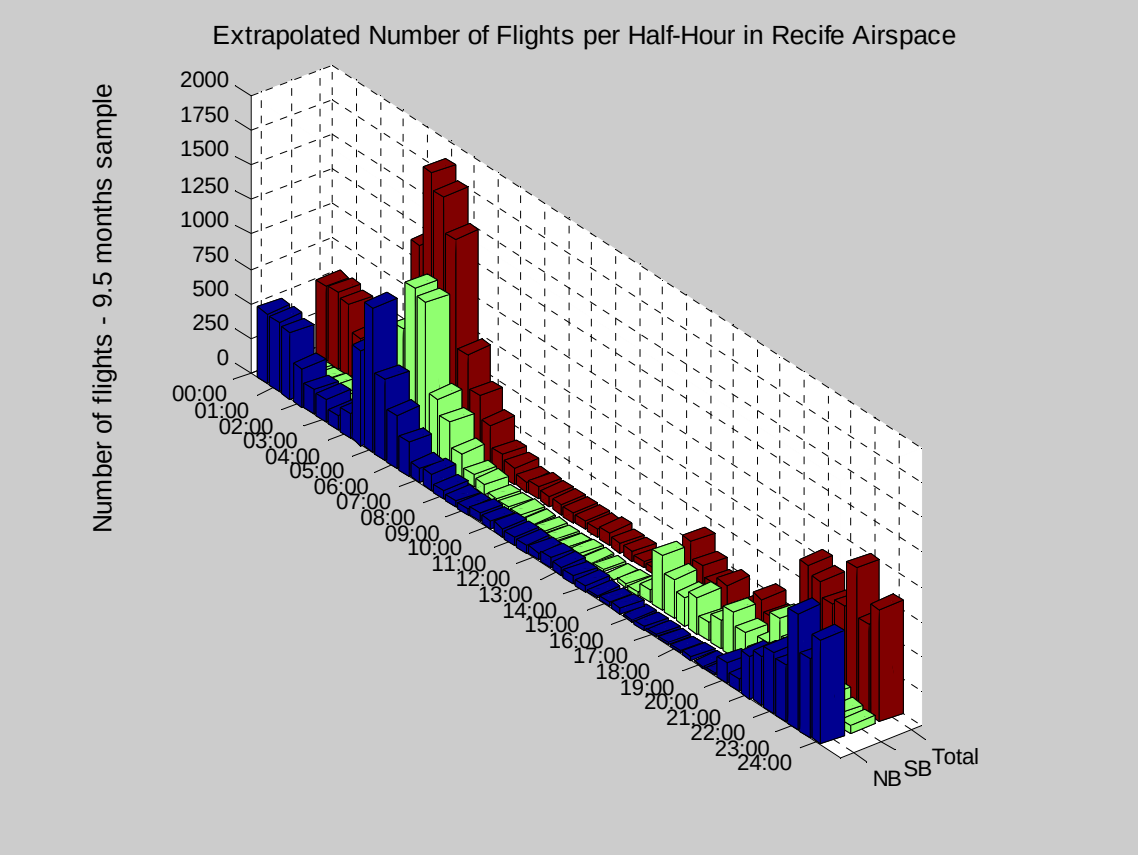

Figure 8
Extrapolated number of flights per hour in Recife airspace

In the previous figures the sum of the traffic in the four routes has been represented, distinguishing only between northbound and southbound traffic.

The next two figures show the traffic distribution per hour just for route UN-741. These graphs give information about the number of flights on this route in both directions.

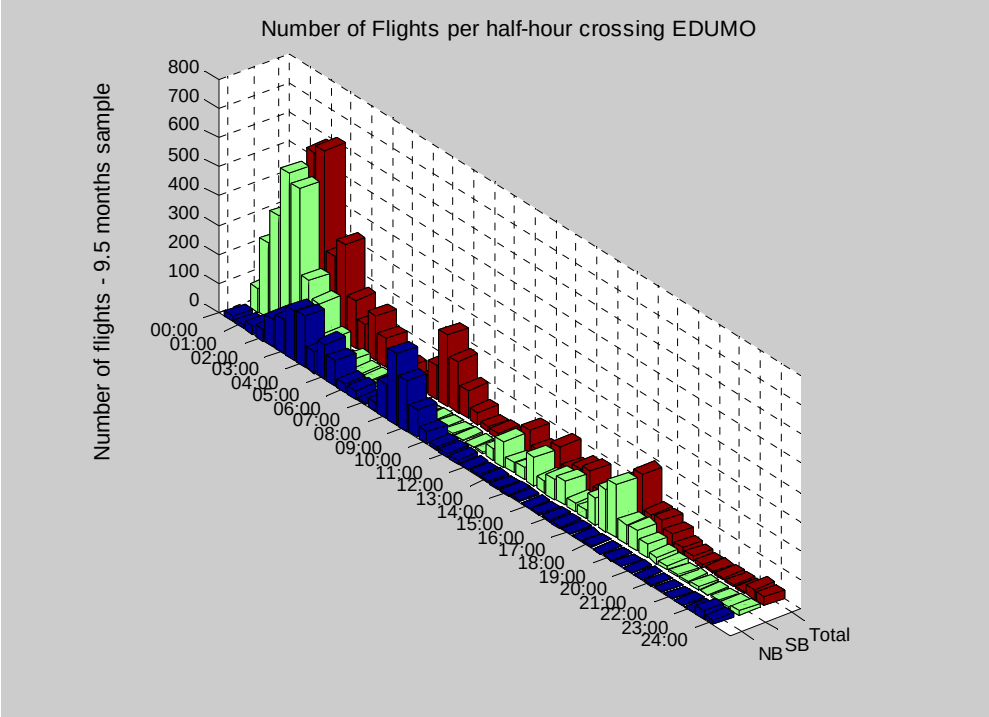

Figure 9
Number of flights per hour for route UN-741 in EDUMO

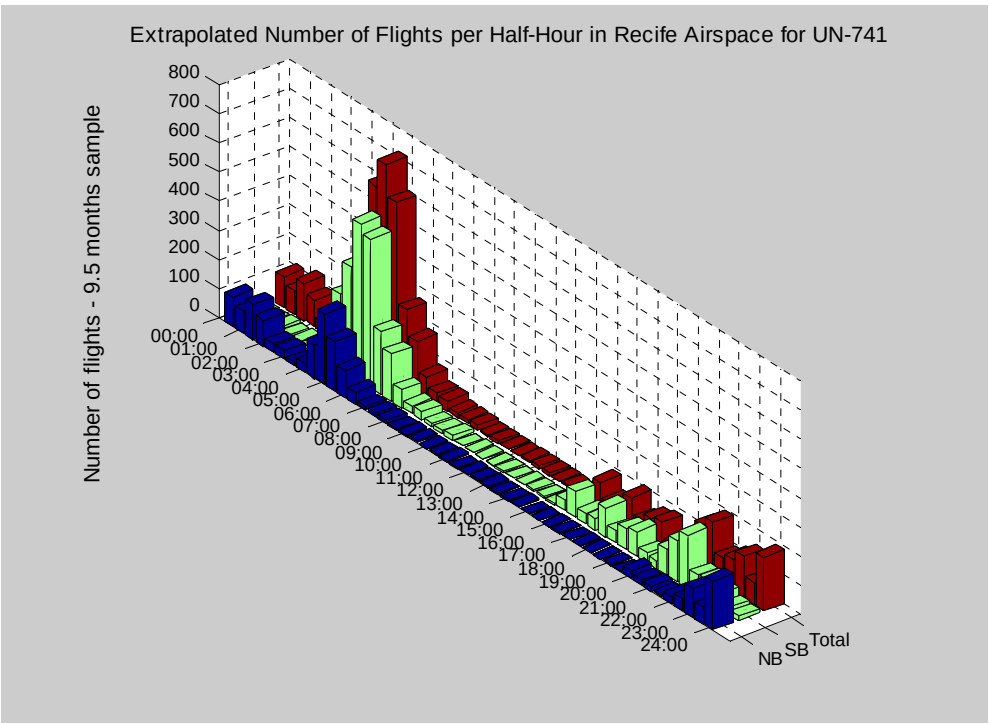

Figure 10
Number of flights per hour for route UN-741 in Recife FIR

Following graphs show the distribution of flights per hour, but just for route UN-866 in this case.

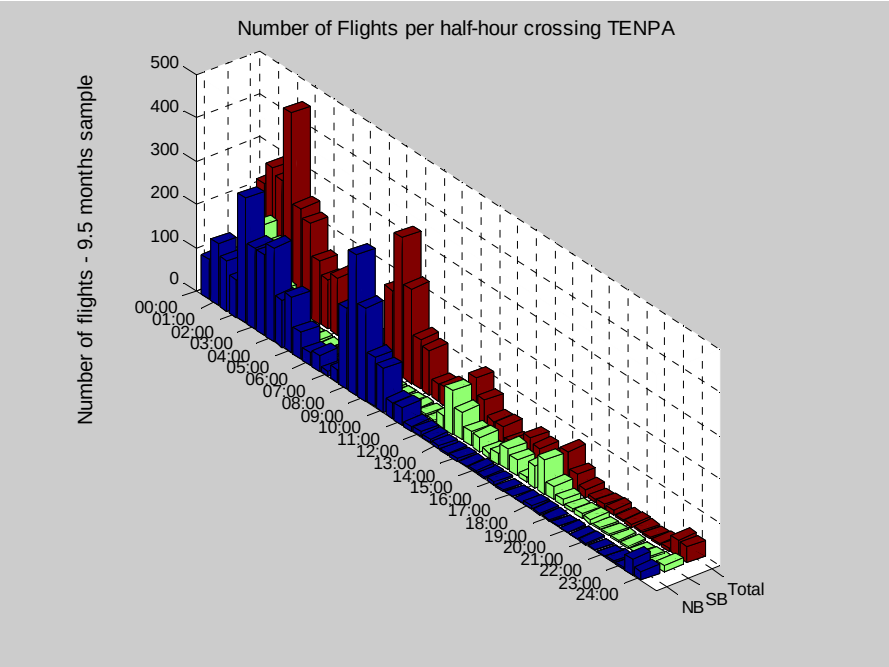

Figure 11
Number of flights per hour for route UN-866 in TENPA

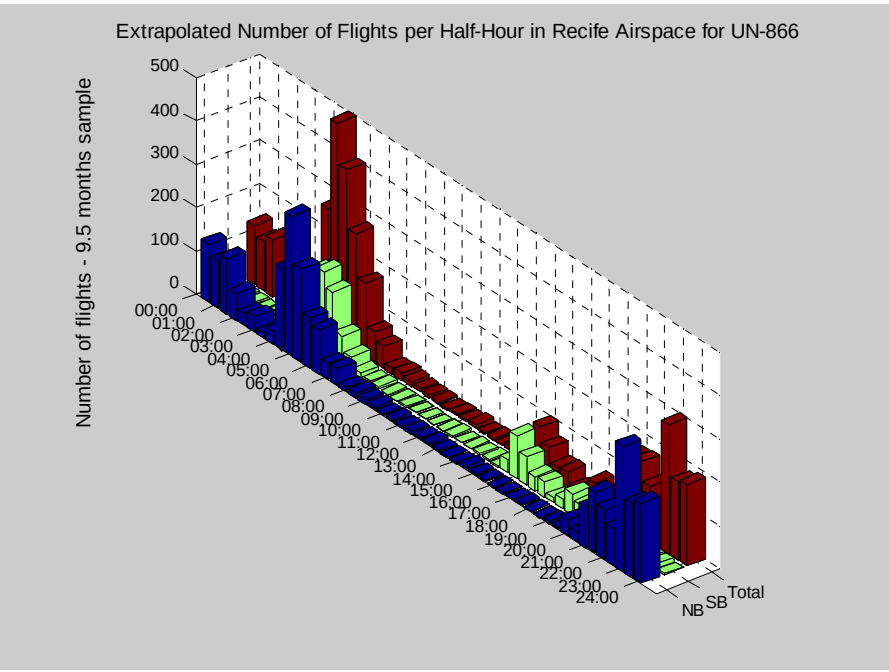

Figure 12
Number of flights per hour for route UN-866 in Recife FIR

The following graphs correspond to route UN-873:

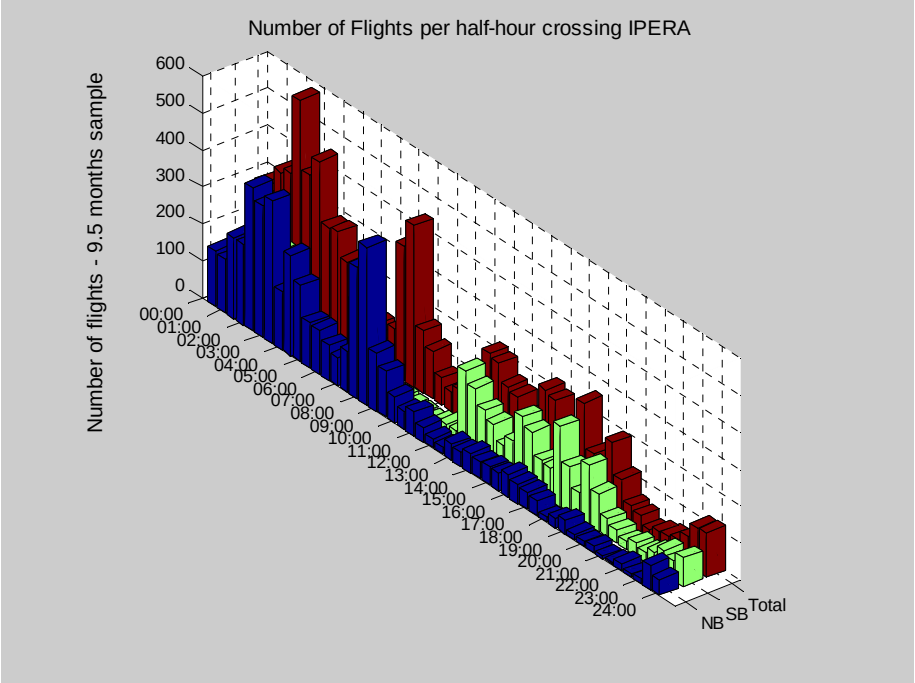

Figure 13
Number of flights per hour for route UN-873 in IPERA

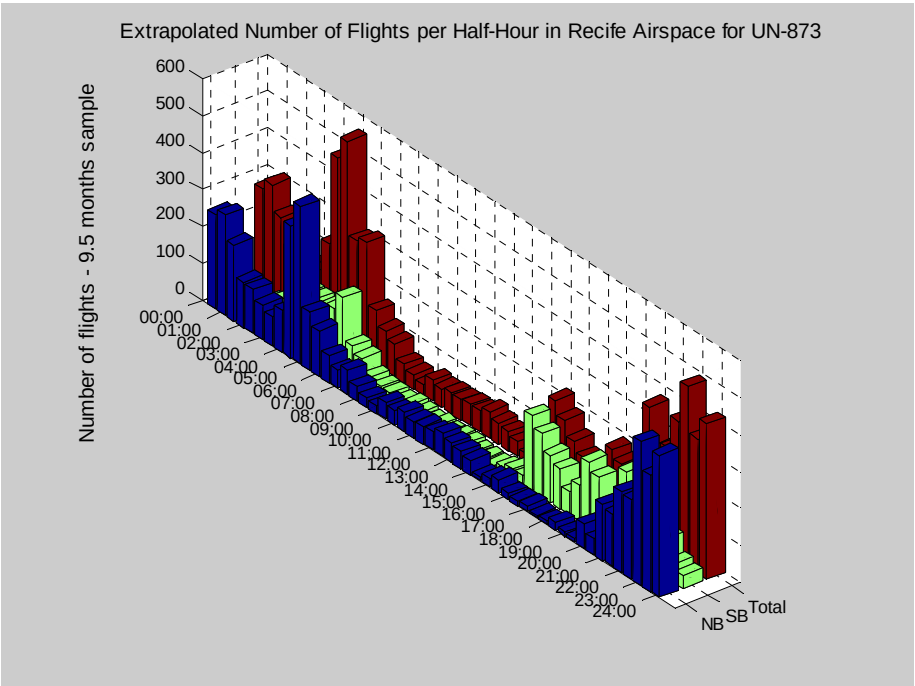

Figure 14
Number of flights per hour for route UN-873 in Recife FIR

And finally, the graphs that correspond to route UN-857:

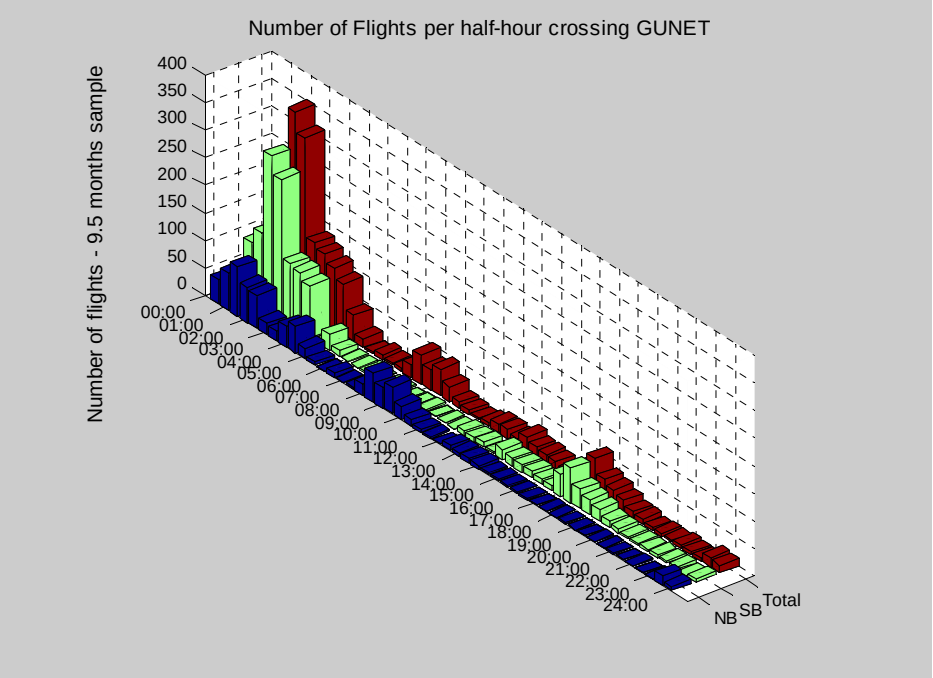

Figure 15
Number of flights per hour for route UN-857 in GUNET

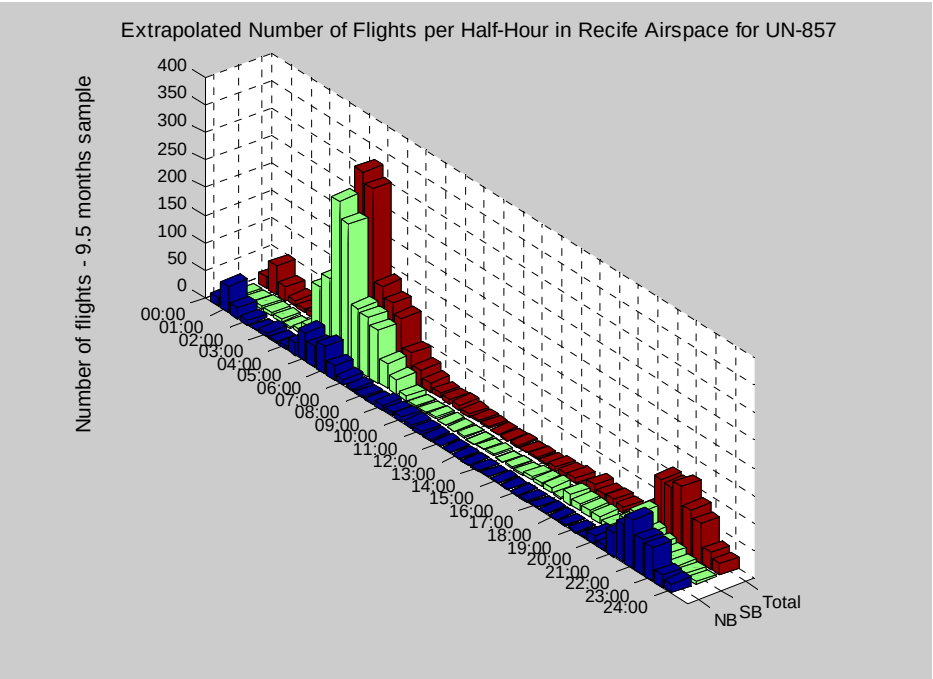

Figure 16
Number of flights per hour for route UN-857 in Recife FIR

3.- LATERAL COLLISION RISK ASSSESSMENT

3.1.- REICH COLLISION RISK MODEL

As the four routes in the EUR/SAM Corridor are nearly parallel, it is possible to use the Reich Collision Risk Model to calculate lateral collision risk.

It models the lateral collision risk due to the loss of lateral separation between aircraft on adjacent parallel tracks flying at the same flight level.

The model reads as follows:

$$N_{ay} = P_y(S_y) \cdot P_z(0) \cdot \frac{\lambda_x}{S_x} \cdot \left\{ E_{y\,same} \cdot \left[\frac{|\Delta \bar{v}|}{2 \cdot \lambda_x} + \frac{|\bar{\dot{y}}|}{2 \cdot \lambda_y} + \frac{|\bar{\dot{z}}|}{2 \cdot \lambda_z} \right] + E_{y\,opposite} \cdot \left[\frac{2.|\bar{v}|}{2 \cdot \lambda_x} + \frac{|\bar{\dot{y}}|}{2 \cdot \lambda_y} + \frac{|\bar{\dot{z}}|}{2 \cdot \lambda_z} \right] \right\}$$

Equation 1

Where:

- N_{ay} is the expected number of accidents (two per each aircraft collision) per flight hour due to the loss of lateral separation between aircraft flying on tracks with nominal spacing S_y.

- S_y is the minimum standard lateral separation.

- $P_y(S_y)$ is the probability of lateral overlap of aircraft nominally flying on laterally adjacent paths at the same flight level.

- $P_z(0)$ is the probability of vertical overlap of aircraft nominally flying at the same flight level.

- E_{ysame} is the same direction lateral occupancy, i.e. the average number of same direction aircraft flying on laterally adjacent tracks at the same flight level within segments of length $2S_x$ centered on the typical aircraft.

- $E_{yopposite}$ is the opposite direction lateral occupancy, i.e. the average number of opposite direction aircraft flying on laterally adjacent tracks at the same flight level within segments of length $2S_x$ centered on the typical aircraft.

- S_x is the length of the longitudinal window used in the calculation of occupancies.

- λ_x is the average length of an aircraft.

- λ_y is the average width of an aircraft.

- λ_z is the average height of an aircraft.

- $\left|\Delta\bar{v}\right|$ is the average relative along-track speed of two aircraft flying at the same flight level in the same direction.

- $\left|\bar{v}\right|$ is the average ground speed of an aircraft.

- $\left|\bar{\dot{y}}\right|$ is the average lateral cross-track speed between aircraft that have lost their lateral separation.

- $\left|\bar{\dot{z}}\right|$ is the average relative vertical speed of aircraft flying at the same flight level.

A collision, and consequently two accidents, can only occur if there is overlap between two aircraft in all three dimensions simultaneously. Equation 1 gathers the product of the probabilities of losing separation in each one of the three dimensions.

As it has already been said, $P_z(0)$ is the probability of vertical overlap; $P_y(S_y)$, the probability of lateral overlap and the combinations $\frac{\lambda_x}{S_x} E_{ysame}$ and $\frac{\lambda_x}{S_x} E_{yopposite}$ relate to the probability of longitudinal overlap of aircraft on adjacent parallel tracks and at the same altitude.

All the probabilities can be interpreted as proportions of flight time in the airspace during which overlap in the pertinent dimension occurs.

As the collision risk is expressed as the expected number of accidents per flight hour, the joint overlap probability must be converted into number of events involving joint overlap in the three dimensions, relating overlap probability with passing frequency[5]. This is achieved by means of the expressions within square brackets in Equation 1. Each of the terms within square brackets represents the reciprocal of the average duration of an overlap in one of the dimensions. For example, $\frac{|\Delta\bar{v}|}{2\lambda_x}$ is the reciprocal of the average duration of an overlap in the longitudinal direction for same direction traffic. In the case of longitudinal direction too, but for opposite direction, the average relative speed is 2v and the average overlap time is $\frac{2|\bar{v}|}{2\lambda_x}$.

The model is based on the following hypothesis:

- All tracks are parallel

- All collisions normally occur between aircraft on adjacent routes, although, if the probability of overlap is significantly large, they may also occur on non-adjacent routes.

[5] Passing frequency between two adjacent routes is the average number of events, per flight hour, in which two aircraft are in longitudinal overlap when travelling in the opposite or same direction at the same flight level

- The entry times into the track system are uncorrelated.
- The lateral deviations of aircraft on adjacent tracks are uncorrelated.
- The lateral speed of an aircraft is not correlated with its lateral deviation.
- The aircraft are replaced by rectangular boxes.
- There is no corrective action by pilots or ATC when aircraft are about to collide.

The model also assumes that the nature of the events making up the lateral collision risk is completely random. This implies that any location within the system can be used to collect a representative data sample on the performance of he system.

As in the analysed airspace there is no opposite direction traffic at the same flight level, due to the flight level orientation scheme, Equation 1 can be simplified as follows:

$$N_{ay} = P_y(S_y) \cdot P_z(0) \cdot \frac{\lambda_x}{S_x} \cdot \left\{ E_{y\,same} \cdot \left[\frac{|\Delta \bar{v}|}{2 \cdot \lambda_x} + \frac{|\bar{\dot{y}}|}{2 \cdot \lambda_y} + \frac{|\bar{\dot{z}}|}{2 \cdot \lambda_z} \right] \right\}$$

Equation 2

In the following sections all the parameters that appear in Equation 1 will be analysed.

3.2.- AVERAGE AIRCRAFT DIMENSIONS: λ_x, λ_y, λ_z

Table 1 shows the dimensions of the various aircraft types found in the SAT during the studied period of time. The average aircraft dimensions have been calculated using the dimensions of each aircraft type and the proportions of flights by type as weighting factors.

The results obtained in this way are:

Dimension	Parameter	Value (ft)	Value (NM)
Length	λ_x	193.39	0.03182
Wingspan	λ_y	179.75	0.02958
Height	λ_z	55.23	0.00909

Table 2
Average airrcraft dimensions

3.3.- PROBABILITY OF VERTICAL OVERLAP: $P_z(0)$

The probability of vertical overlap of aircraft nominally flying at the same flight level of laterally adjacent flight paths is denoted by $P_z(0)$. It is defined by:

$$P_z(0) = \int_{-\lambda_z}^{\lambda_z} f^{z_{12}}(z)dz$$

Equation 3

where $f^{z_{12}}$ denotes the probability density of the vertical distance z_{12} between two aircraft with height deviations z_1 and z_2 nominally at the same flight level, i.e.

$$z_{12} = z_1 - z_2$$

Equation 4

and

$$f^{z_{12}} = \int_{-\infty}^{\infty} f^{TVE}(z_1) f^{TVE}(z_1 - z)dz_1$$

Equation 5

Equation 5 assumes that deviations of the two aircraft are independent and have the same probability density, $f^{TVE}(z_1)$. λ_z denotes the average aircraft height. Substitution of Equation 5 into Equation 3 gives:

$$P_z(0) = \int_{-\lambda_z}^{\lambda_z} \int_{-\infty}^{\infty} f^{TVE}(z_1) f^{TVE}(z_1 - z) dz_1 dz$$

Equation 6

This expression can be approximated by:

$$P_z(0) = 2\lambda_z \int_{-\infty}^{\infty} f^{TVE}(z_1) f^{TVE}(z_1) dz_1$$

Equation 7

Thus, the probability density $f^{TVE}(z_1)$ is needed to calculate $P_z(0)$. It can be taken from section 4.2.5.3 and $P_z(0)$ can be calculated by means of Equation 6. The resulting estimate, based on $\lambda_z = 55.23\ ft$ is $P_z(0) = 0.4308$. This value is less than the value obtained by ARINC in ([Ref. 2]). Therefore, in order to be more conservative, the value used in this study has also been the one obtained by ARINC, i.e. $P_z(0) = 0.57$

3.4.- AVERAGE GROUND SPEED: V

As data on cleared speeds were not provided, speeds and relative velocities have been estimated by comparing waypoint report times. To do this, the CRM program compares the time of waypoint crossing in two waypoints of the track, it calculates the difference between them and multiplies the inverse of this value by the distance that separates those waypoints. The result of this operation is the speed of each aircraft. The average speed, v, is then obtained as the mean value of the speeds of all the aircraft that flew on the four routes during the considered period of time.

As it was previously mentioned, Picasso database contains several errors.
Some errors have been detected in some waypoint crossing times, what leads to extremely high speeds, even impossible in some cases.

As an example, Figure 17 shows speeds of the southbound aircraft that flew in the studied period of time on route UN-741 and on route UN-873.

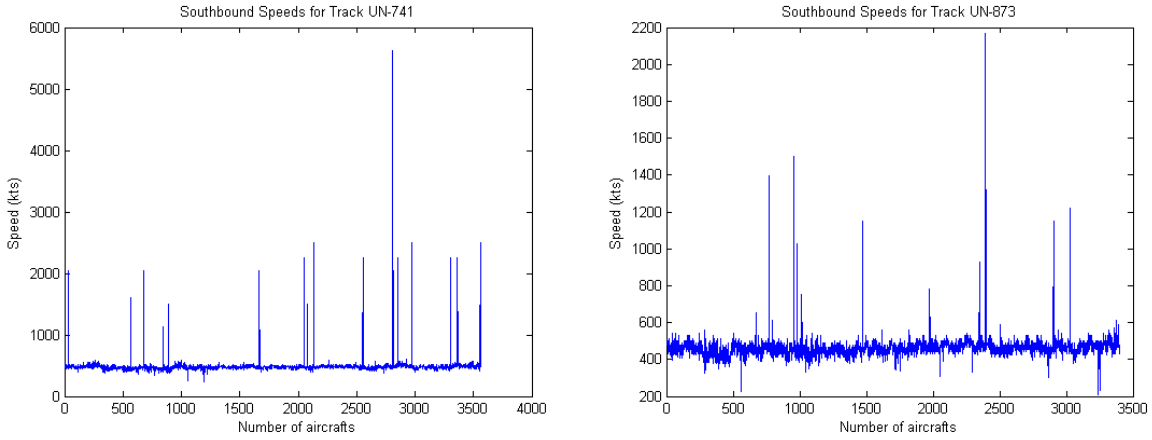

Figure 17
Speeds obtained from Picasso

For example, data from one of the flight plans corresponding to 10th September 2005, identified as the one corresponding to the peak value of more than 4500kts, is shown here:

Indicativo Origen Destino HoraSacta HoraDespegue HoraArribada
VRG8741 EDDF SBGR 10-09-05,06:01:49 - 10-09-05,14:10:00
TipoAeronave ReglasVuelo TipoVuelo Nacionalidad Estela VelCrucero NivelCrucero Matricula
B772 I S I H 493 300 PPVRF
ActivadoTdr EquipoNca ProcDesp ProcArr TrazaRadar
N RWYDSGXI - - S
Hora Preactiv. ATOT IOBT LEOBT CTOT
- - 10-09-05,00:00:00 10-09-05,02:28:00 -
Sectores atravesados : 1
Sector NivelEntrada HoraEntrada HoraSalida NivelEntrada NivelSalida
SW S 10-09-05,06:01:49 10-09-05,06:10:00 330 330
Fijos sobrevolados : 3
Clase Fijo Cx Cy HoraETO NivelPaso TipoETO
1 NELSO 0172725O 0314058N 10-09-05,06:01:49 330 TDR
1 ROSTA 0200000O 0281522N 10-09-05,06:05:02 330 AUTOM.
1 EDUMO 0233600O 0225500N 10-09-05,06:10:00 330 MANUAL
Firs atravesados : 3
Fir HoraEntrada HoraSalida
ACC_CANARIAS 10-09-05,06:01:49 10-09-05,06:10:00
FIR_CANARIAS 10-09-05,06:01:49 10-09-05,06:10:00
FIR_ESPAÑA 10-09-05,06:01:49 10-09-05,06:10:00

According to the flight plan, the distance between ROSTA and EDUMO has been flown in just 4'58'', what leads to such a high speed.

The CRM software tries to correct this problem, limiting the maximum speed. This maximum speed has been fixed in 650 kts. This value is still too high, but it has been taken since it corrects those values that were excessively high and it considers possible anomalous cases in which, because of the characteristics of the aircraft and the existing wind, speeds higher than the habitual ones could be reached.

With this limitation, the speed of each aircraft that flew during the analysed period of time on each route is shown in the following graphs:

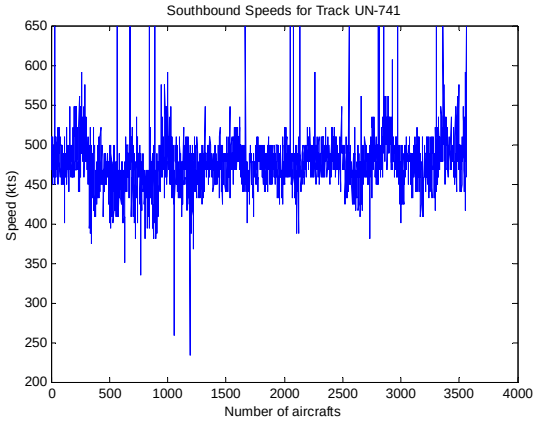
Southbound Speeds for Track UN-741
Speed (kts)
Number of aircrafts

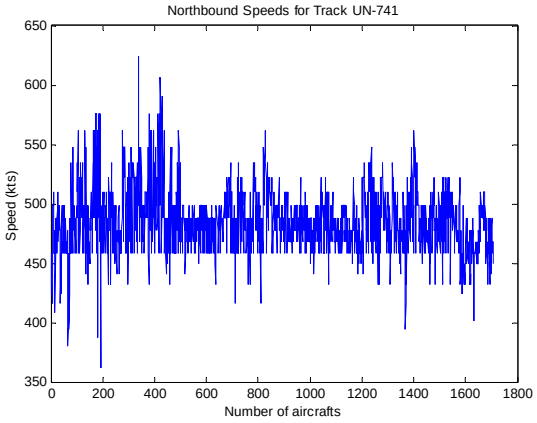
Northbound Speeds for Track UN-741
Speed (kts)
Number of aircrafts

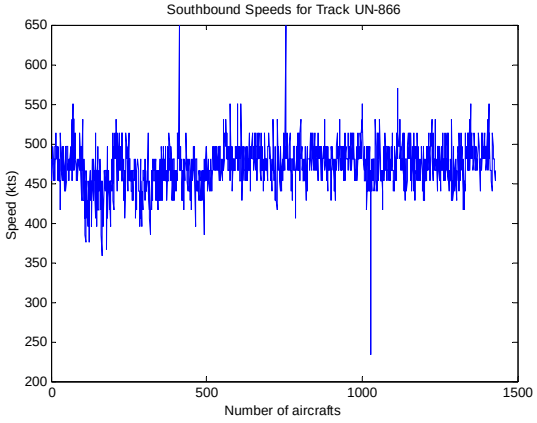
Southbound Speeds for Track UN-866
Speed (kts)
Number of aircrafts

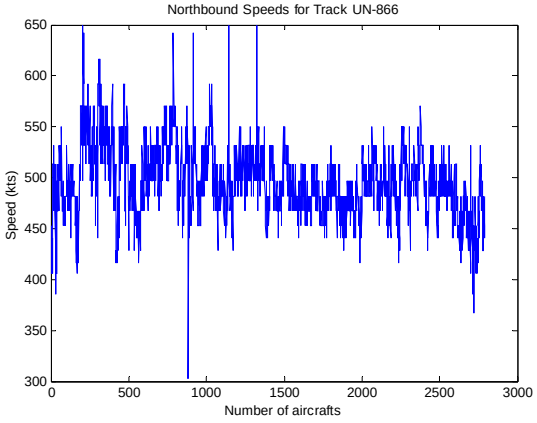
Northbound Speeds for Track UN-866
Speed (kts)
Number of aircrafts

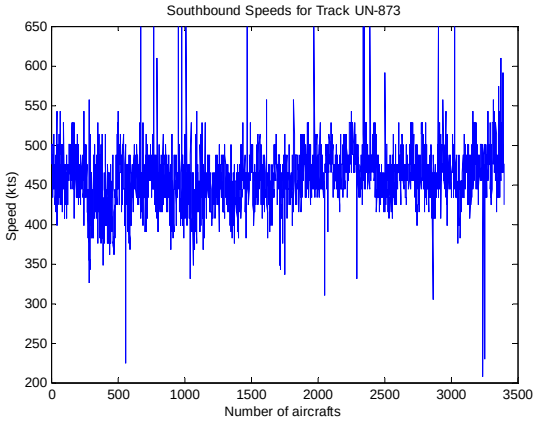
Southbound Speeds for Track UN-873
Speed (kts)
Number of aircrafts

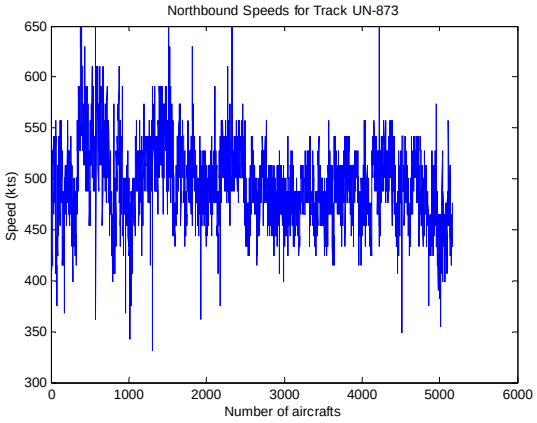
Northbound Speeds for Track UN-873
Speed (kts)
Number of aircrafts

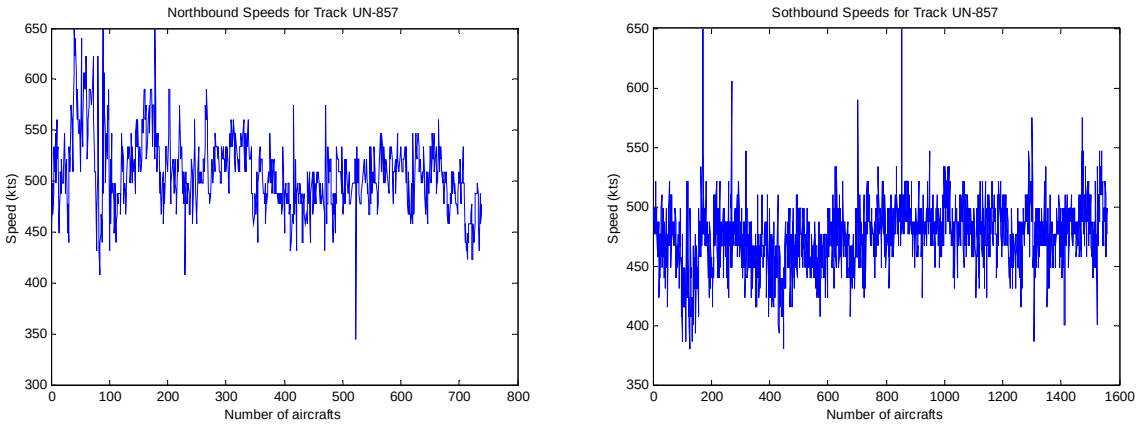

Figure 18
Speeds limited to 650kts

From these speeds, the average ground speed obtained is:

Average Speeds	
Southbound (kts)	467
Northbound (kts)	493
Average (kts)	480

Table 3
Average speed

3.5.- AVERAGE RELATIVE LONGITUDINAL SPEED: ΔV

Δv denotes the average relative longitudinal speed between aircraft flying in the same direction, for it has already been pointed out that in the case of aircraft flying in opposite directions, the average relative longitudinal speed is 2v.

The relative longitudinal speed has been obtained from the differences between the speeds of all the pairs of aircraft that constitute a proximate pair[6] in the same direction. The average relative speed is the mean value of all the calculated differences.

The results obtained are:

Average relative longitudinal speeds	
Southbound (kts)	22.7
Northbound (kts)	26.4
Average (kts)	24.5

Table 4
Average relative longitudinal speed

From these values and in order to be conservative, the value considered for the average relative along-track speed is 26kts.

3.6.- AVERAGE RELATIVE LATERAL SPEED: $\bar{\dot{y}}$

$\left|\bar{\dot{y}}\right|$ is the average relative lateral cross-track speed between aircraft, flying on adjacent routes at the same flight level, that have lost their lateral separation.
The estimation of this parameter generally involves the extrapolation of radar data, speeds and lateral deviations, but such radar data were not available for the current report.

In the study made by ARINC ([Ref. 2]) this value was considered to be $\left|\bar{\dot{y}}\right| = 42kts$, which corresponds to a deviation angle of approximately 5º at an average ground speed of 475-480kts. Although, for example in the North Atlantic (NAT) the value considered was $\left|\bar{\dot{y}}\right| = 80kts$, ARINC thought that this value was too conservative for the SAT. Occurrence of

[6] Lateral proximate pair.- It is defined as an event in which one aircraft on one track passess another aircraft on an adjacent trak at the same level and within a longitudinal distance $2S_x$ ($2T_0$ if it is expressed in time).

waypoint insertion errors and other types of operational errors in the SAT is quite limited, because routes are defined by predetermined fixes, not being necessary to tell their coordinates, which can be misunderstood, but simply its name.

ARINC took this into consideration to reduce the value of $\left|\bar{\dot{y}}\right|$.

In this study, the value considered has also been $\left|\bar{\dot{y}}\right| = 42kts$.

3.7.- AVERAGE RELATIVE VERTICAL SPEED: $\bar{\dot{z}}$

$\left|\bar{\dot{z}}\right|$ denotes the average modulus of the relative vertical speed between a pair of aircraft on the same flight level of adjacent tracks that has lost lateral separation. It is generally assumed that $\left|\bar{\dot{z}}\right|$ is independent of the size of the lateral separation between the aircraft and, for aircraft in level flight, it can also be considered that there is no dependency of $\left|\bar{\dot{z}}\right|$ with the vertical separation between the aircraft.

Data about $\left|\bar{\dot{z}}\right|$ are relatively scarce. Nevertheless, in the study made by ARINC ([Ref. 2]), it was mentioned that data from the NAT showed that $\left|\bar{\dot{z}}\right|$ was of the order of 1kt. From that, ARINC took $\left|\bar{\dot{z}}\right| = 1.5kts$, slightly more conservative. This value has also been considered in this case.

3.8.- LATERAL OVERLAP PROBABILITY: $P_y(S_y)$

The probability of lateral overlap of aircraft nominally flying on adjacent flight paths, separated by S_y, is denoted by $P_y(S_y)$ and it is defined by:

$$P_y(S_y) = \int_{-\lambda_y}^{\lambda_y} f^{y_{12}}(y)dy$$

Equation 8

Where $f^{y_{12}}$ denotes the probability density of the lateral distance y_{12} between two aircraft with lateral deviations y_1 and y_2, nominally separated by S_y, i.e.

$$y_{12} = S_y + y_1 - y_2$$

Equation 9

and

$$f^{y_{12}}(y) = \int_{-\infty}^{\infty} f^{y}(y_1) f^{y}(S_y + y_1 - y) dy_1$$

Equation 10

Equation 10 assumes that the lateral deviations of the two aircraft are independent and have the same probability density, $f^{y}(y_1)$. λ_y denotes the average aircraft width. Substitution of Equation 10 into Equation 8 gives:

$$P_y(S_y) = \int_{-\lambda y}^{\lambda y} \int_{-\infty}^{\infty} f^{y}(y_1) f^{y}(S_y + y_1 - y) dy_1 dy$$

Equation 11

This last equation can be approximated by:

$$P_y(S_y) \approx 2\lambda_y \int_{-\infty}^{\infty} f^{y}(y_1) f^{y}(S_y + y_1) dy_1$$

Equation 12

The probability density function $f^{y}(y_1)$ depends on the nominal and non-nominal navigation capabilities of the aircraft. Nominal navigation performance takes into account typical lateral deviations that arise from ordinary navigational uncertainties when systems are working properly, whilst non-nominal performance represents atypical errors that occur infrequently and that would likely arise from pilot or controller mistakes, or from equipment malfunctions. These atypical errors play an important role in the collision risk, since they may cause large deviations.

The different types of lateral navigation errors are classified as follows according to [Ref. 4] :

Type of error	Description
A	Committed by aircraft not certified for operation in the RNP airspace
B	ATC system loop error
C1	Equipment control error including inadvertent waypoint error
C2	Waypoint insertion error due to the correct entry of incorrect position
D	Other with failure notified to ATC in time for action
E	Other with failure notified to ATC too late for action
F	Other with failure notified/receive by ATC
G	Lateral deviations due to weather when unable to obtain prior ATC clearance

Table 5
Lateral navigation error types

If data of the occurrence of each of these types of errors were available, it would be possible to model the probability density function of the lateral deviations associated to each individual type and to obtain a global distribution by taking a weighted mixture of the individual deviation distributions. The weighting factors would be determined by the frequencies with which the different types of errors occur.

This information was not available for this study, because the only data found correspond to the SATMA (South Atlantic Monitoring Agency) report of June 2002, where the existence of only one lateral deviation (from March to May) of 13.5 NM is notified.

Therefore, to model the probability density function of Equation 12 it is assumed that all lateral errors or deviations follow the same probability distribution. This distribution may then be determined on the basis of a sample of data describing lateral deviations of aircraft from their tracks. It is usually modelled as a mixture of two distributions. These two distributions are:

- The core distribution, which represents errors that derive from standard navigation system deviations. These errors are always present, as navigation systems are not perfect and they have a certain precision.

- The tail distribution, which represents gross navigation errors (GNE), that corresponds to what has been denominated before as non-nominal performance.

It should also be noted that not all atypical errors are large in magnitude and that in most cases it is impossible to determine with certainty if a given observed lateral error arose from the core or from the tail term of the distribution.

Therefore, the overall probability density of lateral navigation errors can be written as:

$$f_y(y_1) = (1-\alpha) \times f_1(y_1) + \alpha \times f_2(y_1)$$

Equation 13

where:

- $f_1(y_1)$ represents the probability density function that models navigation errors arising from typical deviations of the aircraft navigation systems.

- $f_2(y_1)$ represents the probability density function that models lateral navigation errors due to equipment failures, human errors and other atypical errors.

- α represents the percentage of aircraft that experience such anomalies that their distribution of lateral deviations is $f_2(y_1)$.

- (1-α) represents the percentage of aircraft that do not experience such anomalies in their lateral deviations.

To make the tail distribution conservative, the tail distribution is often taken as a double exponential distribution, because of its thick tail.

ARINC also considered a zero mean double exponential distribution for the core term as in the North Pacific collision risk analysis.

The same distribution is used in this study. So,

$$f_1(y_1) = \frac{1}{2a_1}\exp - \left|\frac{y_1}{a_1}\right|$$

Equation 14

$$f_2(y_1) = \frac{1}{2a_2}\exp - \left|\frac{y_1}{a_2}\right|$$

Equation 15

Substituting Equation 14 and Equation 15 in Equation 13:

$$f_y(y_1) = (1-\alpha)\frac{1}{2a_1}\exp - \left|\frac{y_1}{a_1}\right| + \alpha\frac{1}{2a_2}\exp - \left|\frac{y_1}{a_2}\right|$$

Equation 16

The parameter a_1 is determined by the RNP value, since this value indicates that 95% of the deviations are under that value. So, a_1 is obtained solving the following integral:

$$\int_{-RNP}^{RNP} f_1(y_1)dy_1 = 0.95$$

Equation 17

The value for a_1 is then:

$$a_1 = -\frac{RNP}{\log 0.05}$$

Equation 18

Using Equation 18:

a_1	
RNP10	3.338 NM
RNP4	1.335 NM

Table 6
Value of the parameter a_1

As far as the value of a_2 is concerned, in [Ref. 5] it is pointed out that, for a given value of α, $P_y(S_y)$ is maximized taking $a_2 = S_y$. In this case, the minimum separation between tracks is $S_y = 50\text{NM}$, and therefore, $a_2 = 50\text{NM}$.

Knowing a_2, it is possible to obtain the lateral deviations interval within which the aircraft would be with a 95% probability. To do it, the integral of the probability density function is calculated in the unknown interval. The result is a relation between the known parameter a_2 and the maximum unknown lateral deviation that define the 95% interval.

$$\int_{-x}^{x} f_2(y_1)dy_1 = 0.95 \quad \Rightarrow \quad a_2 = -\frac{x}{\log 0.05}$$

Equation 19

Thus, taking $a_2 = 50NM$, 95% of the lateral deviations will be within the interval [-150,150] NM.

The remaining parameter to be fixed in order to define the probability density function completely is α.

This parameter may be interpreted as the probability of an individual aircraft experiencing an anomaly resulting in its distribution of lateral deviations having the scale factor a_2, instead of a_1, or as the proportion of aircraft experiencing anomalies in their lateral navigation performance.

A derivation for the estimate of the weighting factor α used in the study made by ARINC can be found in Appendix A of the cited study ([Ref. 2]). Assuming that one aircraft experiencing a lateral navigation anomaly has been observed, ARINC obtained the value of α from:

$$\alpha = 1 - 0.05^{1/n}$$

Equation 20

where n is the annual number of flights, being $n = 22255$ in that study.

With all that, the obtained value was $\alpha = 1.346 \times 10^{-4}$. The above mentioned Appendix can be consulted for a detailed explanation of its derivation.

In this case, there is no evidence either of any anomalies leading to large navigation errors. Therefore, the same hypothesis of having one large error in the analysed period could be used and the parameter α is obtained using Equation 20 with $n = 20359$, the number of aircraft detedted in the studied period of time. Thus, $\alpha = 1.4713 \times 10^{-4}$

Once the parameters a_1, a_2 and α are defined, the probability density function of the lateral navigation errors is completely modelled.

Using Equation 12, the lateral overlap probability obtained for the different lateral separations between routes existing in the Corridor are the following:

RNP10; S_{ymin}=50NM; α=1.4713*10^{-4}	
P_y(50)	8.645*10^{-8}
P_y(90)	2.891*10^{-8}
P_y(110)	1.938*10^{-8}
P_y(140)	1.064*10^{-8}

Table 7
Lateral overlap probability for different separations between routes with RNP10

The probability increases when the spacing between the routes decreases, as it was expected.

3.9.- LATERAL OCCUPANCY

In Equation 1 there are two occupancy terms, one for same direction occupancy and another one for opposite direction occupancy.

In the current system there is only same direction occupancy, since the same flight levels are used on all routes for each flight direction.

Same direction occupancy is defined as the average number of aircraft which are, in relation to the typical aircraft:

- flying in the same direction as it;
- nominally flying on tracks one lateral separation standard away;
- nominally at the same flight level as it; and
- within a longitudinal segment centered on it.

The above definition has been expanded to include tracks that are separated by more than one lateral separation standard because there is a significant collision risk arising from the probability of overlap between non adjacent tracks.

The length of the longitudinal segment , $2S_x$, is usually considered to be the length equivalent to 20 minutes of flight at 480kts. It has been verified that the relationship between S_x and the occupancy is quite linear.

A similar set of criteria can be used to define opposite direction occupancy, just replacing "flying in the same direction as it" by "flying in the opposite direction".

Occupancy, in general, relates to the longitudinal overlap probability and can be obtained from:

$$E_y = \frac{2T_y}{H}$$

Equation 21

Where:

- T_y represents the total proximity time generated in the system.

- H represents the total number of flight hours generated in the system during the considered period of time.

In Equation 21, the factor 2 allows the conversion of number of collisions into number of accidents.

Two methods can be used to calculate occupancies: “steady state flow model” and “direct estimation from time at waypoint passing”.

In this study the method used has been the second one. This method calculates the number of proximate pairs comparing the time at which aircraft on one route pass a waypoint with the time at which aircraft on a parallel route pass the homologous waypoint. When the difference between passing times is less than certain value, 10 minutes in this case, it is considered that there is a proximate pair in that pair of routes.

Then, occupancy can be calculated using the following expression:

$$E_y = \frac{2n_y}{n}$$

Equation 22

Where n_y is the number of proximate pairs and n is the total number of aircraft.

A more detailed explanation of each method can be found in Annex 1.

As lateral overlap probability depends on lateral spacing between routes and, as it has been said in section 2.- , routes in the EUR/SAM Corridor are not equally spaced, the term $P_y(S_y)E_{ysame}$ in Equation 2 must be split into several terms.

It can be seen in Table 7 that $P_y(90)$ is about 33% of $P_y(50)$, $P_y(110)$ is about 22% of $P_y(50)$ and $P_y(140)$ is about 12% of $P_y(50)$. So, their contributions to the lateral collision risk cannot be ignored and Equation 2 should be written as follows:

$$N_{ay} = \left\{P_y(110).E_{y_{same}} + P_y(90).E^{*}_{y_{same}} + P_y(50).E^{**}_{y_{same}} + P_y(140)E^{***}_{y_{same}}\right\}.P_z(0).\frac{\lambda_x}{S_x}\left\{\frac{|\Delta v|}{2\lambda_x} + \frac{|\dot{\bar{y}}|}{2\lambda_y} + \frac{|\dot{\bar{z}}|}{2\lambda_z}\right\}$$

Equation 23

Where E_{ysame} denotes occupancy for routes UN-741/UN-866; E^*_{ysame}, occupanacy for routes UN-866/UN-873; E^{**}_{ysame}, occupancy for routes UN-873/UN-857 and E^{***}_{ysame}, occupancy for routes UN-866/UN-857.

Therefore, these four same direction occupancy values must be computed.

3.9.2.- Traffic growth hypothesis

This study presents the current collision risk calculated from data corresponding to 2005, but it also presents an estimate of the collision risk over a 10 years horizon.
To do that, it is necessary to know which are the traffic forecasts for that period of time in the studied airspace.

The ASIN study, ([Ref. 10]), considers a moderate scenario with an annual traffic growth rate of 4% and an optimistic scenario with an annual traffic growth of 7%, taking into account the data given by STATFOR-Eurocontrol. Thus, these two cases are analysed here.

3.9.3.- Lateral occupancy values obtained

This section presents the same direction lateral occupancy values provided by the CRM programme for the current time and an estimate of the occupancy until 2015, with the two annual traffic growth rates indicated before, 4% and 7%.

Table 8 shows the number of aircraft and the number of same direction proximate pairs detected on the four routes from 22nd January 2005 till 6th November 2005.

The number of aircraft detected on route RANDOM are also indicated in this table, although they have not been considered in the collision risk estimation.

Number of flights on UN-741	5271
Number of flights on UN-866	4222
Number of flights on UN-873	8569
Number of flights on UN-857	2297
Total number of flights (excluding flights on route RANDOM)	20359
Number of flights on route RANDOM (South-North)	513
Number of aircraft on route RANDOM (North-South)	531
Number of proximate pairs for tracks UN-741/UN-866	414
Number of proximate pairs for tracks UN-866/UN-873	751
Number of proximate pairs for tracks UN-873/UN-857	331
Number of proximate pairs for tracks UN-866/UN-857	216

Table 8
Lateral occupancy parameters

From these data, the occupancies are the ones shown in Table 9:

Lateral occupancy: Year 2005	
Same direction occupancy for UN-741/UN-866	0.0407
Same direction occupancy for UN-866/UN-873	0.0738
Same direction occupancy for UN-873/UN-857	0.0325
Same direction occupancy for UN-866/UN-857	0.0212

Table 9
Lateral occupancies in 2005

Assuming an annual traffic growth rate of 4%, the occupancies for the next 10 years are summarized in Table 10. It holds that occupancy is approximately proportional to traffic flow rate:

4% annual traffic growth	2005	2007	2009	2011	2013	2015
Same direction lateral occupancy for UN-741/UN-866	0,0407	0,0440	0,0476	0,0515	0,0557	0,0602
Same direction lateral occupancy for UN-866/UN-873	0,0738	0,0798	0,0863	0,0934	0,1010	0,1092
Same direction lateral occupancy for UN-873/UN-857	0,0325	0,0351	0,0380	0,0411	0,0445	0,0481
Same direction lateral occupancy for UN-866/UN-857	0,0212	0,0229	0,0248	0,0268	0,0290	0,0314

Table 10
Lateral occupancy estimate until 2015 with an annual traffic growth rate of 4%

If the annual traffic growth rate is 7%, the occupancy values are the ones shown in Table 11:

7% annual traffic growth	2005	2007	2009	2011	2013	2015
Same direction lateral occupancy for UN-741/UN-866	0,0407	0,0466	0,0533	0,0611	0,0699	0,0748
Same direction lateral occupancy for UN-866/UN-873	0,0738	0,0845	0,0967	0,1107	0,1268	0,1357
Same direction lateral occupancy for UN-873/UN-857	0,0325	0,0372	0,0426	0,0488	0,0558	0,0597
Same direction lateral occupancy for UN-866/UN-857	0,0212	0,0243	0,0278	0,0318	0,0364	0,0390

Table 11
Lateral occupancy estimate until 2015 with an annual traffic growth rate of 7%

3.10.- LATERAL COLLISION RISK

Once all the parameters of Equation 23 are obtained, it is posible to calculate the lateral collision risk. This value must not exceed the maximum allowed, for which the system is considered to be safe. This threshold, denominated TLS (Target Level of Safety), has been set to $TLS = 5 \times 10^{-9}$. It means that 5×10^{-9} accidents per flight hour are accepted.

In the current system, with four routes and RNP10, the collision risk values obatained until 2015, with an annual traffic growth rate of 4%, are the ones show in Table 12 and in Figure 19.

Lateral Collision Risk (4% annual traffic growth)	
2005	1,62E-09
2006	1,69E-09
2007	1,75E-09
2008	1,82E-09
2009	1,90E-09
2010	1,97E-09
2011	2,05E-09
2012	2,13E-09
2013	2,22E-09
2014	2,31E-09
2015	2,40E-09

Table 12
Lateral collision risk for the period 2005-2015 with RNP10 and an annual traffic growth rate of 4%

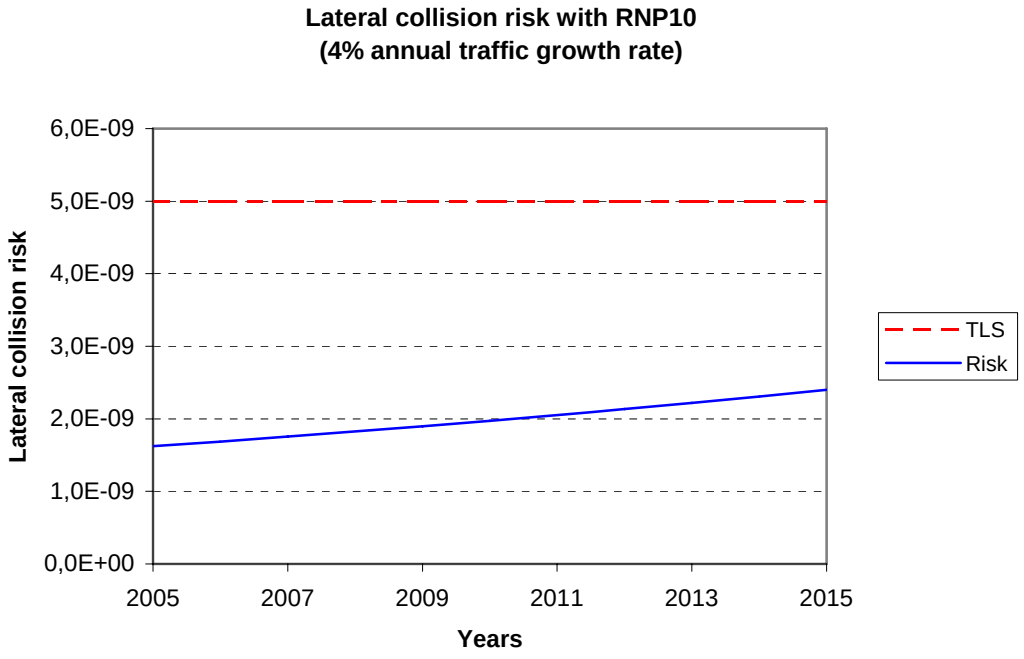

Figure 19
Lateral collision risk for the period 2005-2015 with RNP10 and an annual traffic growth rate of 4%

In the case of a 7% annual traffic growth rate, the resuts are the ones that appear in Table 13 and in Figure 20:

Lateral Collision Risk (7% annual traffic growth)	
2005	1,62E-09
2006	1,74E-09
2007	1,86E-09
2008	1,99E-09
2009	2,13E-09
2010	2,28E-09
2011	2,43E-09
2012	2,60E-09
2013	2,79E-09
2014	2,98E-09
2015	3,19E-09

Table 13
Lateral collision risk for the period 2005-2015 with RNP10 and an annual traffic growth rate of 7%

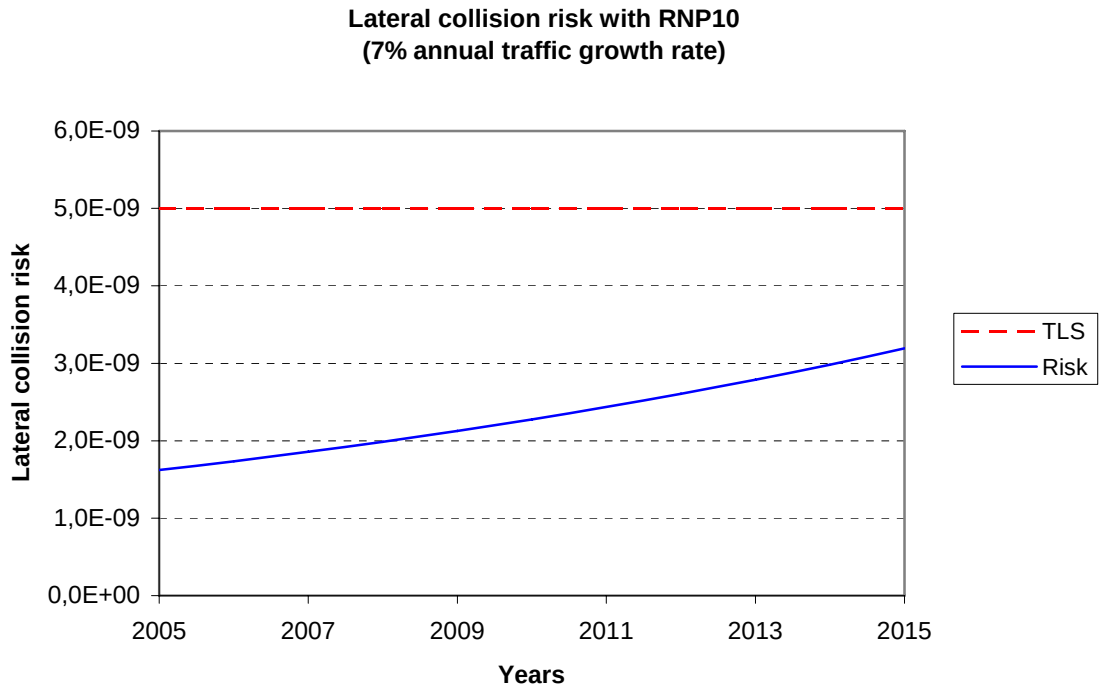

Figure 20
Lateral collision risk for the period 2005-2015 with RNP10 and an annual traffic growth rate of 7%

It can be seen that the EUR/SAM Corridor is laterally safe, since lateral collision risk is below $TLS = 5 \times 10^{-9}$ with the current traffic flow. It is estimated that it will continue to be laterally safe until 2015 with an annual traffic growth rate of 4% and even with an annual traffic growth rate of 7%.

Although traffic on the RANDOM route has not been considered, the current system is considered to be laterally safe, because lateral collision risk is quite far from the maximum allowed and traffic on the RANDOM route is scarce, compared to traffic on the other routes.

4.- VERTICAL COLLISION RISK ASSESSMENT

4.1.- INTRODUCTION

Vertical collision risk, i.e. the risk due to the loss of vertical separation between aircraft on adjacent flight levels is generally made up of three traffic components, namely same direction traffic, opposite direction traffic and crossing traffic.

Vertical collision risk models for same and opposite direction traffic are similar to those for lateral collision risk presented before. They apply to aircraft in straight and level flight. This condition can be assumed to be satisfied within the EUR/SAM Corridor. Nevertheless, some operational causes of height deviations may lead to an aircraft climbing or descending through other flight levels, requiring a different type of modelling.

There are two requirements that must be achieved to consider the airspace vertically safe. They are the following ones:

- In accordance with ICAO Guidance Material, [Ref. 11], the risk of mid-air collision in the vertical dimension within RVSM airspace, due to technical height keeping

performance, shall meet a Target Level of Safety of $2.5*10^{-9}$ fatal accidents per flight hour.

- In accordance with ICAO Guidance Material, [Ref. 11], the management of the overall vertical collision risk within RVSM airspace shall meet a Target Level of Safety of $5.0*10^{-9}$ fatal accidents per flight hour.

In the following sections, the technical vertical risk and the overall vertical risk are assessed.

4.2.- TECHNICAL VERTICAL RISK ASSESSMENT

Technical vertical risk is attributable to the height-keeping errors that result from the combination of altimetry system errors (ASE) and autopilot performance in the vertical dimension.

4.2.1.- Collision Risk Model

The Reich model used for lateral collision risk can also be applied to calculate vertical collision between aircraft on adjacent flight levels of the same track, flying in either the same or the opposite direction. In this case the model is expressed by this equation:

$$N_{aZ} = P_Z(S_Z) \cdot P_Y(0) \cdot \frac{\lambda_x}{S_x} \cdot E_{z\,same} \left[\frac{|\Delta\bar{v}|}{2 \cdot \lambda_x} + \frac{|\bar{\dot{y}}|}{2 \cdot \lambda_y} + \frac{|\bar{\dot{z}}|}{2 \cdot \lambda_z} \right] +$$

$$+ P_z(S_z) \cdot P_y(0) \cdot \frac{\lambda_x}{S_x} \cdot E_{z\,opposite} \cdot \left[\frac{2 \cdot |\bar{v}|}{2\lambda_x} + \frac{|\bar{\dot{y}}|}{2\lambda_y} + \frac{|\bar{\dot{z}}|}{2\lambda_z} \right]$$

Equation 24

Where:

- N_{az} is the expected number of accidents (two per each aircraft collision) per flight hour due to the loss of vertical separation.

- S_z is the vertical separation minimum.

- $P_z(S_z)$ is the probability of vertical overlap of aircraft nominally flying on adjacent flight levels of the same track.

- $P_y(0)$ is the probability of lateral overlap of aircraft nominally flying on the same track.

- E_{zsame} is the same direction vertical occupancy, i.e. the average number of same direction aircraft flying on adjacent flight levels of the same track within segments of length $2S_x$ centered on the typical aircraft.

- $E_{zopposite}$ is the opposite direction vertical occupancy, i.e. the average number of opposite direction aircraft flying on adjacent flight levels of the same track within segments of length $2S_x$ centered on the typical aircraft.

- S_x is the length of the longitudinal window used in the calculation of occupancies.

- λ_x is the average length of an aircraft.

- λ_y is the average width of an aircraft.

- λ_z is the average height of an aircraft.

- $\left|\Delta\vec{v}\right|$ is the average relative along-track speed of two aircraft flying on the same track in the same direction.

- $|\bar{v}|$ is the average ground speed of an aircraft.

- $|\bar{y}|$ is the average lateral cross-track speed between aircraft flying on the same track.

- $|\bar{z}|$ is the average relative vertical speed of aircraft flying on the same track.

As can be seen from Equation 24, the elements of the collision risk model for same and opposite direction traffic are the probabilities of overlap and the average durations of overlaps in the different co-ordinate directions. In the model for same and opposite direction traffic, overlap of two aircraft is defined as overlap of rectangular boxes enveloping the aircraft. It is also assumed that during a situation of overlap, the sides of the boxes remain parallel.

Similar elements play a part in a model of vertical collision risk on crossing routes, but in a more complicated way. Due to the geometry of a crossing, the sides of the rectangular boxes enveloping the aircraft will not be parallel during a situation of horizontal overlap. As a result, the estimation of the average duration of an overlap becomes more complicated. This problem has been addressed by modelling the aircraft by cylinders and calculating the average duration of an overlap from the overlap of the circular cross sections of the cylinders. The diameter of the cylinders is taken as the larger of the length and the wingspan of the aircraft.

Another difference to take into account is that, for a pair of crossing routes, the probability of horizontal overlap cannot be factored into the probabilities of overlap in the longitudinal and lateral directions.

The vertical collision risk model for crossing routes on the basis of the cylindrical aircraft model can be expressed as:

$$N_{aZ} = P_Z(S_Z) \cdot \frac{\lambda_x}{S_{xy}} \cdot E_z(\theta) \left\{ \frac{v_{rel}(\theta)}{\frac{\pi}{2}\lambda_{xy}} + \frac{|\dot{z}|}{2\lambda_z} \right\}$$

Equation 25

Where the relative velocity $v_{rel}(\theta)$ is given by:

$$v_{rel}(\theta) = |\bar{v}|\sqrt{2(1-\cos\theta)}$$

Equation 26

Equation 26 assumes the same average speed for both aircraft.

The new parameters are:

- θ, the angle between two crossing routes, i.e. the angle between the aircraft headings.
- λ_{xy}, the average diameter of a cylinder representing an aircraft.
- S_{xy}, a parameter used for the calculation of $E_z(\theta)$ values.
- $E_z(\theta)$, twice the probability of horizontal overlap of circles representing horizontal cross sections of aircraft on crossing routes.
- $V_{rel}(\theta)$, the average relative speed between aircraft flying on crossing routes.

When there are several pairs of crossing routes with different crossing angles θ_i, i=1,….,n, the model can be applied to each pair of routes and combined subsequently to give:

$$N_{aZ} = P_Z(S_Z) \cdot \frac{\lambda_x}{S_{xy}} \cdot \sum E_z(\theta_i) \left\{ \frac{v_{rel}(\theta_i)}{\frac{\pi}{2}\lambda_{xy}} + \frac{|\dot{z}|}{2\lambda_z} \right\}$$

Equation 27

When the number of crossing angles is relatively large, Equation 27 can be approximated by the model of Equation 25 by taking conservative estimates of $E_z(\theta_i)$ and $v_{rel}(\theta_i)$ valid for each value of i, i=1,….,n.

The vertical collision risk model for crossing tracks can be combined with the model for same and opposite direction traffic to give the complete technical vertical collision risk model for the RVSM safey assessment for the EUR/SAM Corridor in the SAT, i.e.

$$\begin{aligned} N_{aZ} &= P_z(S_z) \cdot P_y(0) \cdot \frac{\lambda_x}{S_x} \cdot E_{zsame} \left[\frac{|\Delta\overline{v}|}{2 \cdot \lambda_x} + \frac{|\overline{\dot{y}}|}{2 \cdot \lambda_y} + \frac{|\overline{\dot{z}}|}{2 \cdot \lambda_z} \right] + \\ &+ P_z(S_z) \cdot P_y(0) \cdot \frac{\lambda_x}{S_x} \cdot E_{opposite} \left[\frac{2 \cdot |\overline{v}|}{2 \cdot \lambda_x} + \frac{|\overline{\dot{y}}|}{2 \cdot \lambda_y} + \frac{|\overline{\dot{z}}|}{2 \cdot \lambda_z} \right] + \\ &+ P_z(S_z) \frac{\lambda_{xy}}{S_{xy}} \sum_{i=1}^{i=n} E_z(\theta_i) \left[\frac{v_{rel}(\theta_i)}{\frac{\pi}{2}\lambda_{xy}} + \frac{|\overline{\dot{z}}|}{2\lambda_z} \right] \end{aligned}$$

Equation 28

In [Ref. 2], ARINC identified four locations where aircraft were crossing the EUR/SAM traffic flow. The crossing angles for these four crossing routes were 89º, 85º, 85º and 77º. These angles were all approximated by 90º angles, reducing Equation 28 to:

$$N_{aZ} = P_z(S_z) \cdot P_y(0) \cdot \frac{\lambda_x}{S_x} \cdot E_{zsame}\left[\frac{|\Delta\bar{v}|}{2 \cdot \lambda_x} + \frac{|\bar{\dot{y}}|}{2 \cdot \lambda_y} + \frac{|\bar{\dot{z}}|}{2 \cdot \lambda_z}\right] +$$
$$+ P_z(S_z) \cdot P_y(0) \cdot \frac{\lambda_x}{S_x} \cdot E_{opposite}\left[\frac{2 \cdot |\bar{v}|}{2 \cdot \lambda_x} + \frac{|\bar{\dot{y}}|}{2 \cdot \lambda_y} + \frac{|\bar{\dot{z}}|}{2 \cdot \lambda_z}\right] +$$
$$+ P_z(S_z) \frac{\lambda_{xy}}{S_{xy}} E_z(90)\left[\frac{|\bar{v}|\sqrt{2}}{\frac{\pi}{2}\lambda_{xy}} + \frac{|\bar{\dot{z}}|}{2\lambda_z}\right]$$

Equation 29

For a 90º crossing angle, the aircraft may be represented by rectangular boxes and it may be assumed that the sides of the boxes remain parallel during a situation of horizontal overlap. The duration of the overlap in each of the two dimensions involved is given by:

$$t_{90} = 2 \times \frac{\frac{\lambda_x}{2} + \frac{\lambda_y}{2}}{|\bar{v}|} = \frac{\lambda_x + \lambda_y}{|\bar{v}|}$$

Equation 30

Substitution of its reciprocal into a model for 90º crossing tracks based on rectangular boxes gives:

$$N_{aZ} = P_z(S_z) \cdot P_y(0) \cdot \frac{\lambda_x}{S_x} \cdot E_{zsame}\left[\frac{|\Delta\bar{v}|}{2 \cdot \lambda_x} + \frac{|\bar{\dot{y}}|}{2 \cdot \lambda_y} + \frac{|\bar{\dot{z}}|}{2 \cdot \lambda_z}\right] +$$
$$+ P_z(S_z) \cdot P_y(0) \cdot \frac{\lambda_x}{S_x} \cdot E_{opposite}\left[\frac{2 \cdot |\bar{v}|}{2 \cdot \lambda_x} + \frac{|\bar{\dot{y}}|}{2 \cdot \lambda_y} + \frac{|\bar{\dot{z}}|}{2 \cdot \lambda_z}\right] +$$
$$+ P_z(S_z) \frac{\lambda_{xy}}{S_{xy}} E_z(90)_{rect}\left[\frac{|\bar{v}|}{\lambda_x + \lambda_y} + \frac{|\bar{v}|}{\lambda_x + \lambda_y} + \frac{|\bar{\dot{z}}|}{2\lambda_z}\right]$$

Equation 31

When the aircraft dimensions from Table 14 are used, the coefficients of $|\overline{v}|$ in the crossing track components of the vertical collision risk models of Equation 29 and Equation 31 are found to be 28.294 and 32.573, respectively. This suggests that the rectangular box model might be slightly more conservative for a 90º crossing angle.

4.2.2.- Average aircraft dimensions: λ_x, λ_y, λ_z

Table 2 showed the average aircraft dimensions for the lateral collision risk model. Clearly, the same dimensions apply to the vertical model. In addition, the vertical model for crossing traffic needs the average diameter of a cylinder enveloping the aircraft. Table 14 shows the pertinent average aircraft dimensions.

Dimension	Parameter	Value (ft)	Value (NM)
Length	λ_x	193.39	0.03182
Wingspan	λ_y	179.75	0.02958
Height	λ_z	55.23	0.00909
Diameter	λ_{xy}	193.39	0.03182

Table 14
Average aircraft dimensions for the vertical collision risk model

4.2.3.- Probability of lateral overlap: $P_y(0)$

The probability of lateral overlap for aircraft nominally flying at adjacent flight levels of the same path is denoted by $P_y(0)$. It is defined by:

$$P_y(0) = \int_{-\lambda_y}^{\lambda_y} f^{y_{12}}(y)dy$$

Equation 32

Where $f^{y_{12}}(y)$ denotes the probability density of the lateral distance y_{12} between two aircraft with lateral deviations y_1 and y_2, nominally at the same track, i.e.

$$y_{12} = y_1 - y_2$$

Equation 33

and

$$f^{y_{12}}(y) = \int_{-\infty}^{\infty} f^{y}(y_1) f^{y}(y_1 - y) dy_1$$

Equation 34

Equation 34 assumes that the deviations of the two aircraft are independent and have the same probability density. λ_y denotes the average aircraft width.

Substitution of Equation 34 into Equation 32 gives:

$$P_y(0) = \int_{-\lambda y}^{\lambda y} \int_{-\infty}^{\infty} f^{y}(y_1) f^{y}(y_1 - y) dy_1 dy$$

Equation 35

This last equation can be approximated by:

$$P_y(0) \approx 2\lambda_y \int_{-\infty}^{\infty} f^{y}(y_1) f^{y}(y_1) dy_1$$

Equation 36

The probability density $f^{Y}(y_1)$ was described in 3.8.- . Using that function in Equation 36, the resulting estimate based on $\lambda_y = 179.75\, ft$ is $P_y(0) = 0.0044$.

This factor has a significant effect on the risk estimate. Therefore, it should not be underestimated. $P_y(0)$ will increase as the lateral navigational performance of typical aircraft improves, causing a corresponding increase in the collision risk estimate. The RGCSP was aware of this problem and attempted to account for improvements in

navigation systems when defining the RVSM global system performance specification. Based on the performance of highly accurate area navigation systems observed in European airspace, which demonstrated lateral path-keeping errors with a standard deviation of 0.3NM, the RGCSP adopted a value of 0.059 as the value of $P_y(0)$ for the global system performance.This value has been used in this study.

4.2.4.- Relative velocities

Equation 31 contains four relative speed parameters, $2|\bar{v}|$, $|\Delta v|$, $|\bar{\dot{y}}|$ and $|\bar{\dot{z}}|$.

The average along track speeds $2|\bar{v}|$ and $|\Delta v|$ are taken the same as for the lateral collision risk model.

For the vertical collision risk model, $|\bar{\dot{y}}|$ is the mean of the modulus of the relative cross-track speed between aircraft on the same track. Consequently, there is no operational reason why this relative speed should have a particularly large value. In the RVSM Safety Asessment of the Australian Airspace, [Ref. 13], the value considered for this parameter was 13kts. A more conservative value, 20kts, was used by ARINC in [Ref. 2]. This value has been taken here too.

The mean relative vertical speed of the vertical collision risk model applies to aircraft that have lost their assigned vertical separation minimum of S_z. The value $|\bar{\dot{z}}| = 1.5\,kts$ will be taken here as in the lateral collision risk assessment..

4.2.5.- Vertical overlap probability: $P_z(S_z)$

The probability of vertical overlap of a pair of aircraft nominally flying at adjacent flight levels separated by S_z is denoted $P_z(S_z)$. It is defined by:

$$P_z(S_z) = \int_{-\lambda_z}^{\lambda_z} f^{z_{12}}(z)dz$$

Equation 37

Where $f^{z_{12}}(z)$ denotes the probability density of the vertical distance z_{12} between the two aircraft. This distance may be defined as:

$$z_{12} = S_z + z_1 - z_2$$

Equation 38

with z_1 and z_2 representing the height-keeping deviations of two aircraft. Height-keeping deviations of aircraft are usually defined in terms of Total Vertical Error (TVE), measured in geometric feet:

$$TVE = actual\ \ pressure\ altitude\ \ flown\, by\, an\, aircraftt - assigned\ \ altitude$$

Assuming that the height-keeping deviations of the two aircraft are independent and denoting their probability densities by $f_1^{TVE}(z_1)$ and $f_2^{TVE}(z_2)$, the probability density $f^{z_{12}}(z)$ and the probability of vertical overlap can be written as:

$$f^{z_{12}}(z) = \int_{-\infty}^{\infty} f_1^{TVE}(z_1) f_2^{TVE}(S_z + z_1 - z)dz_1$$

Equation 39

$$P_z(S_z) = \int_{-\lambda z}^{\lambda z} \int_{-\infty}^{\infty} f_1^{TVE}(z_1)\, f_2^{TVE}(S_z + z_1 - z)dz_1 dz$$

Equation 40

This equation can be approximated by:

$$P_z(S_z) \approx 2\lambda_z \int_{-\infty}^{\infty} f_1^{TVE}(z_1) f_2^{TVE}(S_z + z_1) dz_1$$

Equation 41

The probability distribution of the height-keeping deviations, $f^{TVE}(z)$, depends on the height-keeping characteristics of the aircraft as specified by the MASPS. Data on the height-keeping performance of MASPS-approved aircraft can be obtained by means of aircraft height monitoring. Currently, height monitoring data are not available from the SAT. However, as the majority of the aircraft types and operators in the EUR/SAM Corridor are also flying in the European RVSM height monitoring program, these data will be used.

$f^{TVE}(z)$ can be obtained modelling separately the two components of TVE: Altimetry System Error (ASE) and Flight Technical Error (FTE):

$$TVE = ASE + FTE$$

Equation 42

where

$$ASE = actual\ pressure\ altitude\ flown\ by\ an\ aircraft - displayed\ altitude$$

$$FTE = displayed\ altitude - assigned\ altitude$$

Assuming that the two components are statistically independent:

$$f^{TVE}(z) = \int_{-\infty}^{\infty} f^{ASE}(a) f^{FTE}(z - a) da$$

Equation 43

In practice, FTE is difficult to determine and it is approximated by Assigned Altitude Deviation (AAD):

$$AAD = transponded\ altitude - assigned\ altitude$$

Equation 43 can then be approximated by:

$$f^{TVE}(z) = \int_{-\infty}^{\infty} f^{ASE}(a) f^{AAD}(z-a) da$$

Equation 44

The difference between FTE and AAD is referred to as correspondence error. It arises due to the rounding of the altimeter reading before transmission by the aircraft transponder. Data on AAD can be obtained by evaluating archived mode C data.

Figure 21 shows a diagram of the components of the Total Vertical Error:

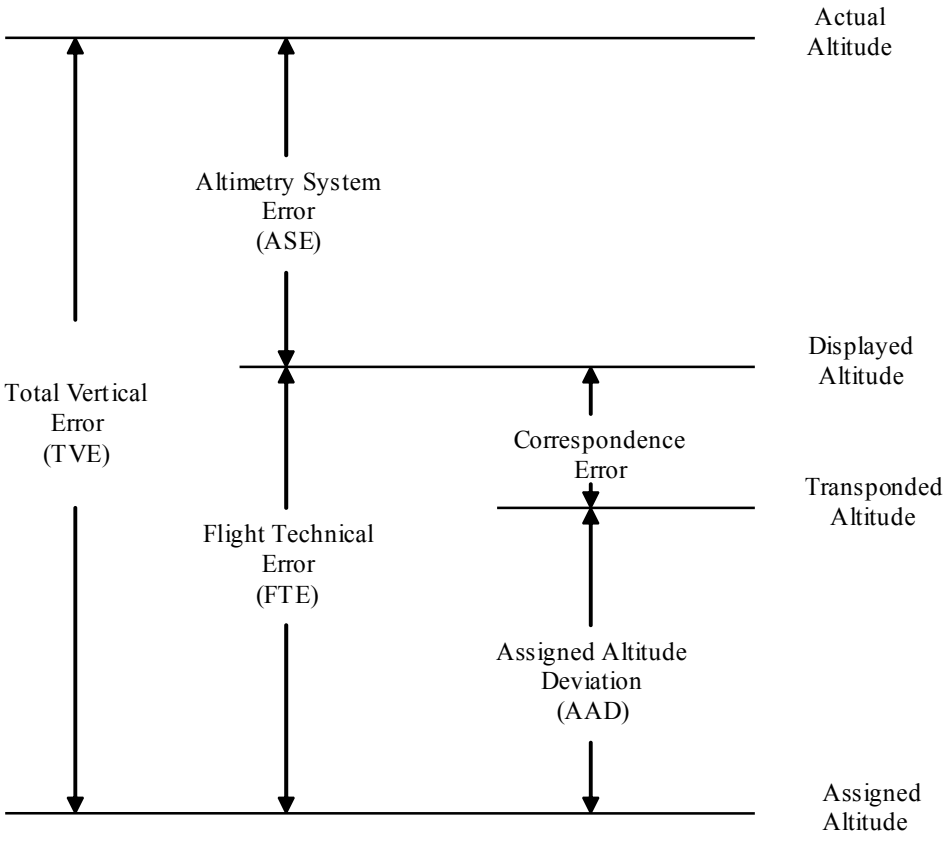

Figure 21
Breakdown of height-keeping errors

The modelling of the two component densities, ASE and AAD, is described below.

4.2.5.1.- ASE Distribution Modelling

The overall ASE distribution is a combination of ASE distributions for each aircraft monitoring classification, weighted by the proportion of flights made by the classification, i.e.

$$f^{ASE}(a) = \sum_{i=1}^{n_{tg}} \beta_i f_i^{ASE}(a)$$

Equation 45

where n_{tg} denotes the number of different aircraft type groups, β_i is the proportion of flight time contributed by aircraft type group i and $f_i^{ASE}(a)$ is the probability density of the ASE of aircraft type group i, i=1,…..,n_{tg}.

The probability densities $f_i^{ASE}(a)$ are to be determined on the basis of height monitoring data of MASPS approved aircraft. As it was mentioned before, such monitoring data are not available from the SAT. Therefore, in this study, the probability density functions obtained based on data from the European and NAT height monitoring programs are used. To be more precise, the probability density functions used are those presented in Table 3-8 of the "EUR RVSM Report 2005", [Ref. 12], presented in the 32nd Meeting of the MDG.

In the cited report, [Ref. 12], the ASE measurements used to derive the ASE distribution fit for each monitoring group was a combination of continental HMU data with data from the HMU located at Strumble. Nevertheless, the statistical anlysis of ASE measurements from the different HMUs showed significant differences of Strumble measurements with respect to the EUR HMUs, which led to

a much higher overlap probability. Therefore, until those differences were clarified, it was decided to discard data from Strumble for that report.

While this study is being elaborated, it has been known that in the final version of the cited report, the Strumble data have been finally used and that there may be some differences between the ASE probability density functions presented in the MDG 32 and the final ones. However, it has not been possible to have access to those final distributions for this study. This must be taken into account, and the values obatained here should be reviewed when more data are available.

Table 15 shows the proportion of flight time and the ASE probability density of each aircraft type of the 38 aircraft types with higher proportion of flight time. The remaining 40 types are not included because of their rare occurrence. The proportions of flight time from the second column of Table 15 have been re-normalized to ensure that the weighting factors β_i add up to one.

In the third column of Table 15, GDE stands for Gaussian-Double Exponential and G, for Gaussian distribution. The pdf of a GDE distribution is:

$$f_i^{ASE}(x) = (1-\alpha)\frac{1}{s_1\sqrt{2\pi}}\exp\left[-\frac{1}{2}\left(\frac{x-m}{s_1}\right)^2\right] + \alpha\frac{1}{2b}\exp\left[-\left|\frac{x-m}{b}\right|\right]$$

Equation 46

$$b = s_2/\sqrt{2}$$

Equation 47

Aircraft Type	Proportion of flight time	Type of pdf	Mean (ft)	s(ft) (G/DE only)	s_1 (ft) (GDE only)	s_2 (ft) (GDE only)	α (ft) (GDE only)
B777-200	0.1527	GDE	28	0	32.60	50.84	0.4343
A340-300	0.1340	GDE	-6.28	0	38.02	59.65	0.5755
MD11	0.1110	GDE	-10.93	0	52.91	56.02	0.1449
B767-300	0.1000	GDE	-66.92	0	46.66	48.03	0.3562
A310	0.0978	GDE	-56.7	0	57.98	60.86	0.5976
B747-400	0.0910	GDE	-60.14	0	38.74	42.61	0.2629
A330-200	0.0672	GDE	44.34	0	39.44	46.48	0.5051
A340-600	0.0579	GDE	33.7	0	31.40	43.33	0.1854
B757-200	0.0530	GDE	-8.84	0	38.53	54.92	0.4732
B747-200	0.0337	GDE	-36.98	0	58.99	62.95	0.3060
A320-100	0.0178	GDE	37.00	0	44.41	48.43	0.2722
A320	0.0153	GDE	36.99	0	44.41	48.43	0.2722
A330-300	0.0112	GDE	44.34	0	39.44	46.48	0.5051
A340-200	0.0107	GDE	-6.28	0	38.02	59.65	0.5755
B737-800	0.0096	GDE	8.62	0	44.68	48.72	0.2797
DC10	0.0050	GDE	-5.8	0	60.19	65.03	0.1417
B777-300	0.0032	GDE	22.7	0	26.62	28.84	0.3394
F900	0.0031	GDE	30	0	60.93	70.24	0.4307
A340	0.0023	GDE	-6.28	0	38.02	59.65	0.5755
L101	0.0019	GDE	5.2	0	67.04	90.69	0.1729
A319	0.0016	GDE	36.99	0	44.41	48.43	0.2722
E135	0.0014	GDE	-4.81	0	59.19	63.59	0.0754
B737	0.0014	GDE	8.62	0	44.68	48.72	0.2797
B747-300	0.0013	GDE	-36.98	0	58.99	62.95	0.3060
GLF4	0.0012	GDE	-22.4	0	51.89	57.80	0.3432
B707-300	0.0012	G	-0.5	75.32	0	0	0
CL60	0.0012	GDE	-4.6	0	52.49	59.46	0.6291
F2TH	0.0010	GDE	-26.9	0	58.30	63.70	0.1690
H25B	0.0008	GDE	22	0	58.81	79.89	0.3635
B757-300	0.0008	GDE	-7.7	0	39.11	42.70	0.2086
FA50	0.0007	GDE	56.1	0	64.03	64.92	0.2557
E170	0.0007	GDE	110.4	0	45.25	60.90	0.5242
B737-200	0.0007	GDE	44.3	0	36.93	77.28	0.3775
LJ35	0.0006	GDE	64.3	0	44.00	96.49	0.4309
B737-500	0.0006	GDE	-40.1	0	45.42	50.45	0.2458
GLEX	0.0006	GDE	27.2	0	62.89	67.68	0.3748
C750	0.0005	GDE	-7.3	0	45.61	60.73	0.3364
GLF5	0.0004	GDE	5	0	61.63	59.68	0.4086

Table 15
Proportion of flight time and ASE disributions per aircraft type

The mean and the standard deviation of the ASE density function are given by:

$$m\{ASE\} = \sum_{i=1}^{n_{tg}} \beta_i m_i$$

Equation 48

$$s^2\{ASE\} = \sum_{i=1}^{n_{tg}} \beta_i s_i^{\,2} + \sum_{i=1}^{n_{tg}} \beta_i m_i^{\,2} - \left(m\{ASE\}\right)^2$$

Equation 49

where m_i denotes the ASE mean of the i-th aircraft type and s_i denotes the ASE standard deviation of type i. Thus, the mean and standard deviation of the overall ASE density $f^{ASE}(a)$ are -10.31ft and 61.74ft respectively.

4.2.5.2.- AAD Distribution Modelling

AAD performance is subdivided into typical and atypical performance. For the assessment of technical vertical risk, only typical AAD will be taken into account for the AAD component of TVE. All data on atypical AAD will be included in the assessment of the vertical risk due to all causes.

In [Ref. 12] typical AAD performance is taken to be that which is not greater than 350ft in magnitude and any AAD greater than that value is considered to be atypical.

AAD data on typical performance should be obtained from the height monitoring process, while AAD data on atypical performance should be obtained from incident reports.

As no data from the SAT was available for this study, the value obtained in the RVSM Report for 2005 for the European airspace ([Ref. 12]) has been used. The

distribution chosen in that report to model the typical AAD is a Double Exponential (DE), with mean -0.473ft and standard deviation value of 42.82. Its equation is:

$$f^{AAD}(a) = \frac{1}{2b_{AAD}} \exp\left[-\left| \frac{a - m_{AAD}}{b_{AAD}} \right| \right]$$

Equation 50

Where m_{AAD} is the mean value and b_{AAD} is given by Equation 47, substituting s_2 by the standard deviation of the AAD function.

4.2.5.3.- TVE Distribution Modelling

Substitution of the ASE and AAD densities of the foregoing two subsections into Equation 44 yields the TVE density $f^{TVE}(z)$.

The probability of vertical overlap is calculated by means of Equation 41. The resulting value is $P_z(1000) = 1.5447 \times 10^{-9}$.

In addition to the TLS of 2.5×10^{-9} for technical vertical risk, there are some constraints to be met by the TVE performance of aircraft. Firstly, the Global System Performance Specification requires the probability of vertical overlap, $P_z(1000)$, not to be greater than 1.7×10^{-8}. The value obtained does satisfy this requirement.

Appart from this requirement, section 2.3.1 of ICAO Document 9574 (2nd Edition), [Ref. 11], states that the aggregate of Total Vertical Error (TVE) performance in the airspace simultaneously satisfies the following four requirements, constituting the Global Height-Keeping Performance Specification:

- The proportion of TVE beyond 90m (300ft) in magnitude must be less than 2.0×10^{-3}

- The proportion of TVE beyond 150m (500ft) in magnitude must be less than 3.5×10^{-6}

- The proportion of TVE beyond 200m (650ft) in magnitude must be less than 1.6×10^{-7}

- The proportion of TVE between 290 and 320m (950ft and 1050ft) in magnitude must be less than 1.7×10^{-8}

Meeting the criteria of the global height-keeping performance specification provides additional confidence in the estimate of the probability of vertical overlap.

The values obtained with the probability density $f^{TVE}(z)$ used in this study are shown in the following table:

Quantity	Estimate	Upper Bound
$\Pr ob\{\|TVE\| \geq 300\}$	$8.6569*10^{-4}$	$2.0*10^{-3}$
$\Pr ob\{\|TVE\| \geq 500\}$	$5.8087*10^{-6}$	$3.5*10^{-6}$
$\Pr ob\{\|TVE\| \geq 650\}$	$1.9932*10^{-7}$	$1.6*10^{-7}$
$\Pr ob\{950 \leq \|TVE\| \leq 1050\}$	$3.5263*10^{-10}$	$1.7*10^{-8}$

Table 16
Estimates of Proportions of Height-Keeping Errors

The results show that the first and the fourth critera are met, being the remaining criteria only slightly exceeded.

In the safety assessments made for the Asia/Pacific Region, [Ref. 13] and [Ref. 14], the value used for $P_z(1000)$ is the much more conservative value used in the NAT,

i.e. $P_z(1000) = 2.46 \times 10^{-8}$. Therefore, in this study the assessment will be made with both values: $P_z(1000) = 1.5447 \times 10^{-9}$ and $P_z(1000) = 2.46 \times 10^{-8}$.

4.2.6.- Vertical occupancy

Vertical occupancy can be defined for same and opposite direction traffic in the same way as lateral occupancy. Thus, "same direction, single separation minimum vertical occupancy" is the average number of aircraft, which are, in relataion to the typical aircraft:

- flying in the same direction as it;
- nominally on the same track as it;
- nominally flying at flight levels one vertical separation minimum away from it; and
- within a longitudinal segment centered on it, whose length is $2S_x$.

A similar set of criteria can be used to define opposite direction vertical occupancy.

Therefore,

$$E_z = \frac{2T_z}{H}$$

Equation 51

Where

- T_z: The total same (opposite) direction proximity time generated in the system, i.e. the total time spent by same (opposite) direction aircraft pairs on the same

flight paths at adjacent flight levels and within a longitudinal distance S_x of each other; and

- H: The total number of flying hours generated in the system during the period considered.

The same method used to estimate lateral occupancy, "direct estimation from time at waypoint passing", can also be used to estimate same and opposite direction vertical occupancy. In this case, the condition that the points utilized should be approximately on a plane at right angles to the track system is automatically satisfied for aircraft on the same track. Thus, occupancy can be obtained using the following equation:

$$E_z = \frac{2n_z}{n}$$

Equation 52

where n_z is the total number of vertically proximate pairs and n is the total number of aircraft.

Table 17 shows some results on same and opposite vertical occupancy. Same direction vertical occupancy is zero due to the flight level allocation scheme in use.

It was verified that the relationship between S_x and vertical occupancy was linear. The vertical collision risk has been calculated on the basis of $S_x = 80NM$.

Vertical occupancy: Year 2005	
Number of flights on UN-741	5271
Number of flights on UN-866	4222
Number of flights on UN-873	8569
Number of flights on UN-857	2297
Total number of flights (excluding flights on route RANDOM)	20359
Number of opposite direction vertical proximate events for UN-741	89
Number of opposite direction vertical proximate events for UN-866	123
Number of opposite direction vertical proximate events for UN-873	393
Number of opposite direction vertical proximate events for UN-857	57
Total number of opposite proximate events	662
Same direction vertical occupancy (S_x=80NM)	0
Opposite diection vertical occupancy S_x=80NM)	0.0650

Table 17
Vertical occupancy in 2005

Crossing track occupancy may, in principle, be defined in the same way as same and opposite direction vertical occupancy, e.g:

$$E_z(\theta) = \frac{2T_z(\theta)}{H}$$

Equation 53

where $T_z(\theta)$ is the total time spent by aircraft pairs on routes crossing at an angle θ at adjacent flight levels within a distance S_{xy} of eah other.

It may also be estimated by:

$$E_z(\theta) = \frac{2n_z(\theta)}{n}$$

Equation 54

where $n_z(\theta)$ is the total number of vertically proximate pairs on the routes intersecting at an angle θ and n is the total number of aircraft. A way of determining whether or

not an aircraft pair is vertically proximate would be on the basis of the times t_c of passing the crossing point. If the crossing point is not a reporting point for both the aircraft, then interpolated values based on the surrounding reporting points have to be used.

No data on crossing traffic was available for this study. ARINC, in [Ref. 2], obtained the value 0.003471 for the crossing track occupancy corresponding to 2000. Not enough data were available for that study either and some hypothesis had to be made (see [Ref. 2]).

In this case, that value will be used for current traffic levels but multiplied by 1.3 to consider the 5.4% annual traffic growth rate in the EUR/SAM Corridor. Thus, the crossing occupancy taken here is 0.004512. Nevertheless, this value should be reviewed when current data are available.

Once vertical occupancy is calculated based on current traffic levels, it is possible to estimate the occupancy in the following years taking into account the annual traffic growth rate forecasted. Vertical occupancy values from 2005 to 2015 with an annual traffic growth rate of 4% are shown in Table 18.

Year	2005	2007	2009	2011	2013	2015
Opposite direction vertical occupancy	0,0650	0,0703	0,0760	0,08224	0,0889	0,0962
Crossing occupancy	0,0045	0,0049	0,0053	0,0057	0,0062	0,0067

Table 18
Vertical occupancy estimate until 2015 with an annual traffic growth rate of 4%

If the annual traffic growth rate is 7%, the occupancy values are the ones shown in Table 19:

Year	2005	2007	2009	2011	2013	2015
Opposite direction vertical occupancy	0,0650	0,0744	0,0852	0,0975	0,1117	0,1279
Crossing occupancy	0,0045	0,0052	0,0059	0,0068	0,0077	0,0089

Table 19
Vertical occupancy estimate until 2015 with an annual traffic growth rate of 7%

4.2.7.- Technical vertical collision risk

The estimates of the different parameters are summarized in Table 20.

$P_y(0)$	0.059
$P_z(1000)$ (Calculated / NAT)	$1.5447*10^{-9}$ / $2.46*10^{-8}$
λx (NM)	0.03182
λy (NM)	0.02958
λz (NM)	0.00909
$\lvert\bar{v}\rvert$ (kts)	480
$\lvert\dot{\bar{y}}\rvert$ (kts)	20
$\lvert\dot{\bar{z}}\rvert$ (kts)	1.5
S_{xy} (NM)	80
E_z	See Table 18 and Table 19

Table 20
Summary of Vertical Collision Risk Model Parameters

The technical vertical risk is obtained substituting these parameters into Equation 31. As vertical occupancy in the same direction is zero, this equation can be simplified, giving:

$$N_{aZ} = P_z(S_z)\cdot P_y(0)\cdot\frac{\lambda_x}{S_x}\cdot E_{zopposite}\left[\frac{2\cdot|\bar{v}|}{2\cdot\lambda_x}+\frac{|\dot{\bar{y}}|}{2\cdot\lambda_y}+\frac{|\dot{\bar{z}}|}{2\cdot\lambda_z}\right]+$$
$$+P_z(S_z)\frac{\lambda_{xy}}{S_{xy}}E_z(90)_{rect}\left[\frac{|\bar{v}|}{\lambda_x+\lambda_y}+\frac{|\bar{v}|}{\lambda_x+\lambda_y}+\frac{|\dot{\bar{z}}|}{2\lambda_z}\right]$$

Equation 55

Table 21 shows the estimate of the vertical collision risk based on traffic levels projected forward over a ten-year planning horizon, considering that the traffic growth factor is 4% per annum. These results can also be seen in Figure 22

Year	Technical Vertical Collision Risk 4% annual traffic growth	
	$P_z(1000) = 1.5447 \times 10^{-9}$	$P_z(1000) = 2.46 \times 10^{-8}$
2005	8,01E-11	1,28E-09
2006	8,33E-11	1,33E-09
2007	8,66E-11	1,38E-09
2008	9,01E-11	1,44E-09
2009	9,37E-11	1,49E-09
2010	9,75E-11	1,55E-09
2011	1,01E-10	1,61E-09
2012	1,05E-10	1,68E-09
2013	1,10E-10	1,75E-09
2014	1,14E-10	1,82E-09
2015	1,19E-10	1,89E-09

Table 21
Technical Vertical Collision Risk with 4% annual traffic growth

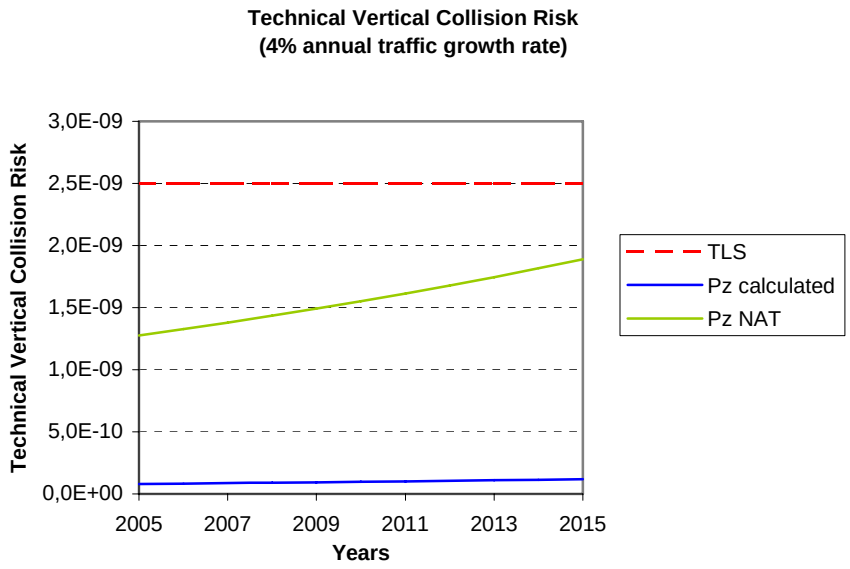

Figure 22
Technical Vertical Collision Risk with 4% annual traffic growth

If the traffic growth factor is 7% per annum, the results are the ones shown in Table 22 and in Figure 23:

Year	Technical Vertical Collision Risk 7% annual traffic growth	
	$P_z(1000) = 1.5447 \times 10^{-9}$	$P_z(1000) = 2.46 \times 10^{-8}$
2005	8,01E-11	1,28E-09
2006	8,57E-11	1,37E-09
2007	9,17E-11	1,46E-09
2008	9,81E-11	1,56E-09
2009	1,05E-10	1,67E-09
2010	1,12E-10	1,79E-09
2011	1,20E-10	1,91E-09
2012	1,29E-10	2,05E-09
2013	1,38E-10	2,19E-09
2014	1,47E-10	2,35E-09
2015	1,58E-10	2,51E-09

Table 22
Technical Vertical Collision Risk with 7% annual traffic growth

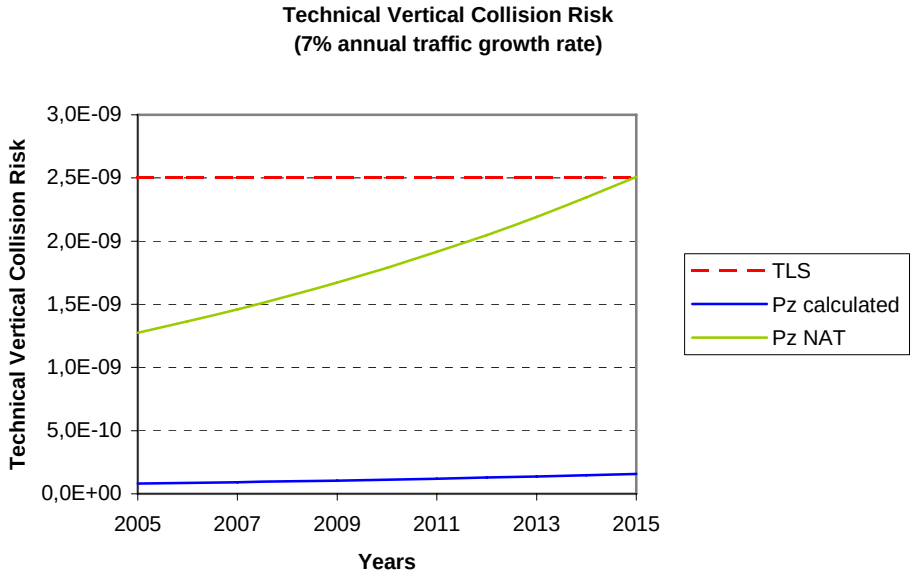

Figure 23
Technical Vertical Collision Risk with 7% annual traffic growth

It can be seen that the estimates of the technical vertical risk are less than the technical TLS for both values of $P_z(1000)$. Only in 2015 and with the conservative overlap probability used in the NAT, the technical risk would be equal to the maximum allowed, considering a 7% annual traffic growth rate.

4.3.- TOTAL VERTICAL RISK ASSESSMENT

In order to assess the total vertical risk, the risk due to large, atypical height deviations must be assessed and added to the technical vertical risk.

Whilst the technical vertical risk for aircraft on non-adjacent flight levels is negligible in comparison with those on adjacent flight levels, the same is not true for the risk due to atypical height deviations.

Atypical height deviations can be due to exceptional technical errors or due to operational errors.

Altitude deviations resulting from exceptional technical errors are subdivided into five categories, according to the cause of deviation. These are:

- Turbulence: Incidents in which an aircraft deviates from its assigned altitude as a result of pressure turbulence, or turbulence from another aircraft.

- TCAS: false RA-TCAS alerts when there is no other aircraft nearby.

- TCAS: nuisance RA-TCAS alerts against an aircraft that is not posing a threat; for example, an aircraft that is climbing to the level below.

- Autopilot failure: the aircraft deviates from its assigned flight level due to a malfunction in the autopilot system.

- Other technical malfunctions: for example, an electrical fault on engine problem.

On the other side, altitude deviations due to operational errors are due to ATC-pilot loop errors and incorrect clearances. These include:

- Climb/descend without ATC clearance.

- Failure to climb/descend as cleared.

- Entry to RVSM airspace at an incorrect level.

- ATC system loop error (e.g. pilot misunderstands clearance or ATC issues incorrect clearance).

Height deviations due to TCAS do not usually involve whole number of flight levels, i.e. climbing or descending through one or more flight levels without clearance or levelling off at a wrong flight level, but may be much larger than the normal deviations of MASPS approved aircraft. However, deviations caused by the remaining types of error may involve whole number of flight levels.

In relation to this, a distinction between large height deviations involving whole numbers of flight levels and large height deviations not involving whole numbers of flight levels was made for the NAT and different models for the associated probabilities of vertical overlap were developed.

For the European risk assessment, a new approach to modelling these types of large height deviations and the corresponding probability of vertical overlap was developed. The new approach differs from the one used in the NAT in that a kind of artificial distribution of AAD

is constructed. It is artificial in that, where appropiate, it takes into account the risk on non-adjacent flight levels as if arcraft were actually at adjacent flight levels. In this way, the new approach unifies the modelling of the vertical collision risk due to large deviations involving and not involving whole numbers of flight levels.

The model used to estimate the risk due to large height deviations differs from the technical vertical risk model only in the computation of the probability of vertical overlap, P_z, and the relative vertical speed, $|\dot{\bar{z}}|$.

The total vertical risk is then obtained as the sum of the technical collision risk and the risk due to atypical deviations.

Following sections describe the modelling of large height deviations used for the European risk assessment. They are literally extracted from section 5.3 of [Ref. 15].

4.3.1.- Modelling of atypical AADs

A large atypical deviation can follow three main paths, which are illustrated in Figure 24.

The figure depicts a scenario where aircraft 1 should climb to a certain flight level. The correct path of the aircraft is shown by the solid line. The three possible types of deviation which aircraft 1 might make are depicted by dotted line paths A, B and C.

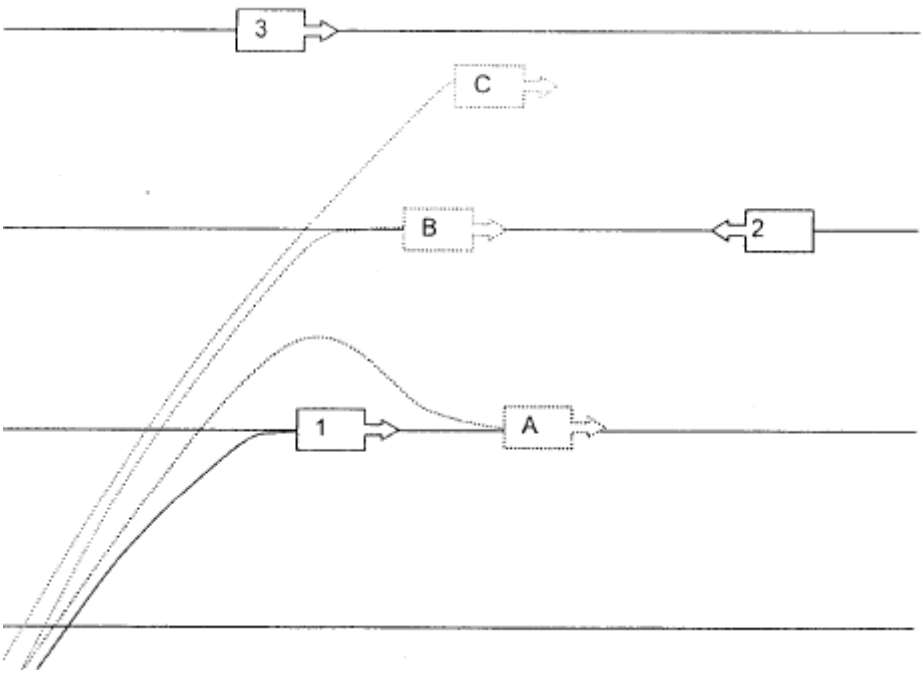

Figure 24
Illustration of the three basic deviation paths

In scenario A, aircraft 1 fails to capture its correct flight level, and performs a height bust. This manoeuvre could result in a loss of separation with aircraft 2 on the adjacent flight level. In addition, although aircraft 1 does not reach the flight level of aircraft 2, there is still a small chance of collision due to the possible errors in the technical height keeping performance of the two aircraft. For example, if the height bust resulted in a nominal Mode C vertical separation of 500ft between the two aircraft, the actual vertical separation could be less (or greater) depending upon the technical height keeping error of the two aircraft.

In scenario B, aircraft 1 climbs to and joins an incorrect flight level. This results in a possibility of collision with aircraft 2, the risk being dependent on the relative horizontal velocity of the two aircraft (i.e. whether they are same or opposite direction traffic) and the length of the time the aircraft spends on the incorrect level without the deviation being corrected in some way, either by a reclearance or return to the correct flight level.

In scenario C, aircraft 1 climbs through an incorrect level. This again results in a possibility of collision with aircraft 2, the risk again being dependent on the relative horizontal velocity of the two aircraft, but also on the climb rate of aircraft 1, since this is directly proportional to the length of time it takes aircraft 1 to pass through the level of aircraft 2. The aircraft could also have a loss of separation with aircraft 3.

The modelling of large height deviations is now described. The modelling is slightly different depending on whether the deviation involved level flight (eg joining an incorrect flight level) or climbing/descending flight (eg commiting a height bust).

4.3.1.1.- Modelling the effect of an individual atypical altitude deviation by a climbing/descending aircraft, where S_z=1000ft.

- Case 1: Altitude deviation is less than S_z:

Consider an aircraft that has a large height deviation of less than the separation standard S_z, as depicted in scenario A of Figure 24. Further suppose that the amounts of time spent at 100-ft deviation intervals, Δt_i, i=1,…..,i_{max} are known, where i_{max} denotes the 100ft interval pertaining to the maximum deviation. If the detailed time history of a large height deviation is not available from the incident report, an approximation can be constructed based on an appropriate constant climb/descent rate.

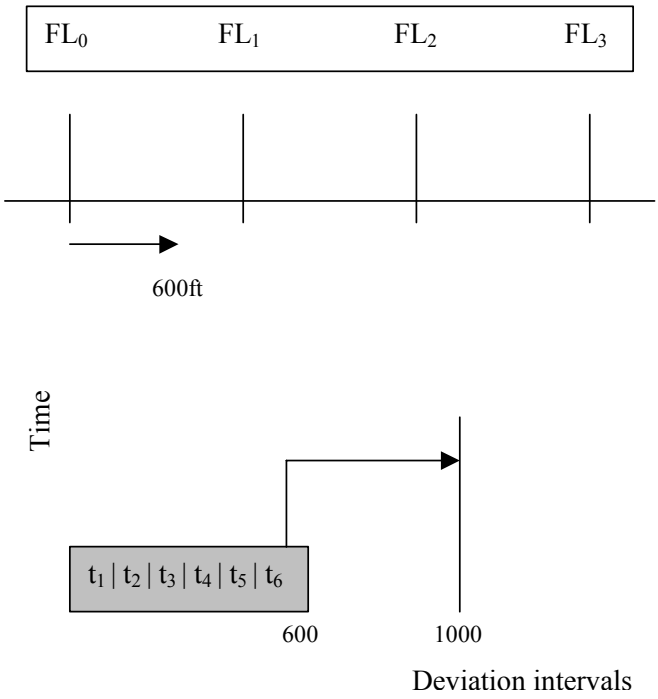

Figure 25
A large AAD of less than one separation standard

This figure depicts a situation where, for example, an aircraft that should have levelled at FL_0 in fact performed a height bust of 600ft. Estimating the risk of collision for this event rests on the idea that for the duration of time spent in the i_{th} 100ft deviation interval, the probability of vertical overlap can be estimated by $P_z(1000\text{-}D_i)$, where D_i is the magnitude of deviation of the i_{th} interval. For example, at the maximum deviation of 600ft in the above scenario, the probability of vertical overlap would be estimated by $P_z(400)$, since the aircraft is at this point at a nominal distance of 400ft away from the next flight level FL_1. Strictly speaking the aircraft also has a risk of overlap with FL_2, equal to $P_z(1400)$ but this is negligible in comparison with $P_z(400)$. In the figure, the duration of time is shown shaded in dark grey.

In practice, $P_z(S_i)$, where $S_i=1000\text{-}D_i$, can be estimated using Equation 41.

- Case 2: Altitude deviation is between S_z and $2S_z$

Consider an aircraft that has a large height deviation of between one and two standard separations, as sketched in Figure 26 and depicted in scenario C of Figure 24. Again suppose that the amounts of time spent at 100-ft deviation intervals, Δt_i, i=1,…..,i_{max} are known, or can be constructed based on appropriate constant climb/descent rate.

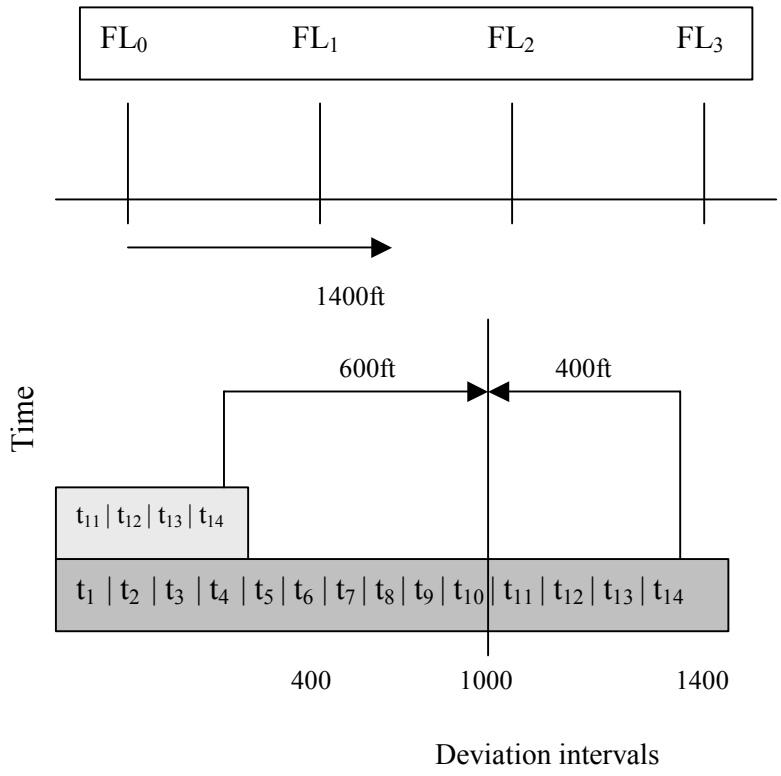

Figure 26
A large AAD of between one and two standard separations

Figure 26 depicts a situation where, for example, an aircraft that should have levelled at FL_0 but in fact mistook its level clearance and performed a height bust of 1400ft. Estimating the risk of collision for this event rests on the idea that for the duration of time spent in the i_{th} 100ft deviation interval, the probability of vertical overlap can be estimated by $P_z(|1000 - D_i|)$ where D_i is

the magnitude of deviation of the i_{th} interval. The absolute value is required in this case because for the time spent in deviation grater than 1000ft, the aircraft is at a separation of D_i-1000 from aircraft on FL_1. However it is also true that for the time spent in deviation greater than 1000ft, the aircraft is at a separation of 2000-D_i, from aircraft on FL_2. To account for this, the time spent in the intervals greater than 1000ft are "added in" to the corresponding intervals between FL_0 and FL_1. Thus, for example, modelling the risk at 1400ft deviation, separated by 600ft from aircraft on FL_2 is performed by adding in the time t_{14} to the time t_4, as if the error were another 400ft deviation, separated by 600ft from aircraft at FL1. This approximation is valid so long as the frequency of horizontal overlap between aircraft on adjacent levels is similar to the frequency of horizontal overlap for non-adjacent flight levels.

If $S_i = |1000 - D_i|$, then the expression for $P_z(S_i)$ can again be estimated using Equation 41.

- Case :3: Altitude deviation greater than $2S_z$

Consider an aircraft that has a large height deviation greater than two standard separations, as sketched in Figure 27. Again suppose that the amounts of time spent at 100-ft deviation intervals, Δt_i, i=1,…..,i_{max} are known, or can be constructed based on an appropriate constant climb/descent rate.

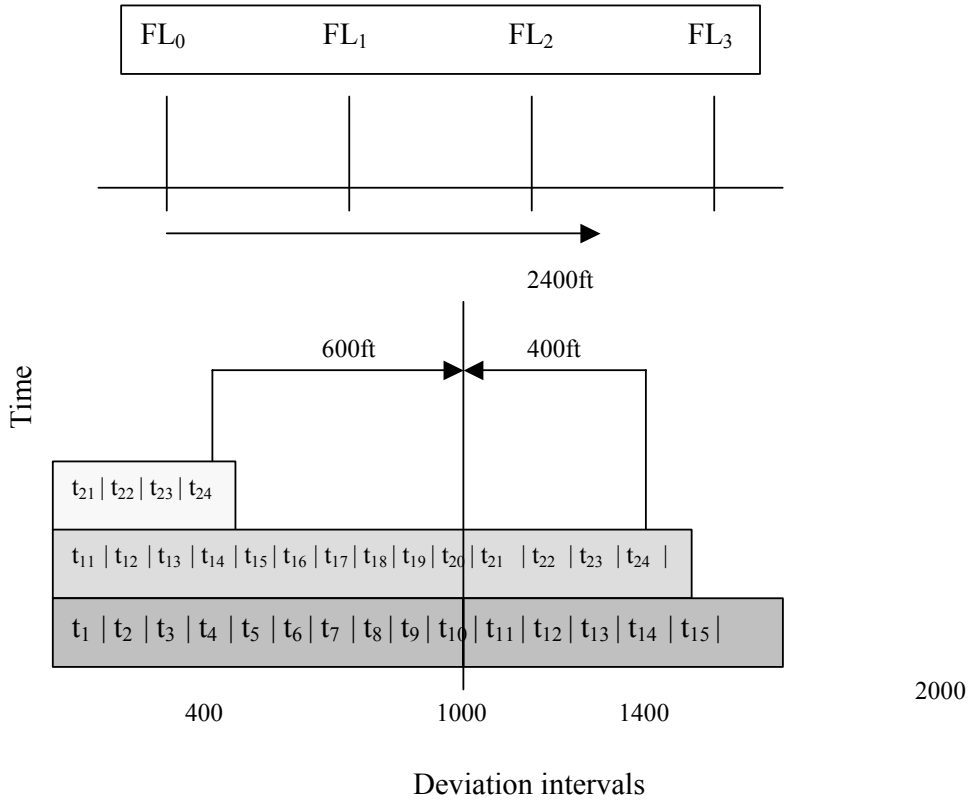

Figure 27
A large AAD of greater than two standard separations

Figure 27 depicts a situation where, for example, an aircraft that should have been at FL_0 in fact acted on the level clearance for another aircraft and performed a height bust of 2400ft. Estimating the risk of collision for this event rests on the idea that for the duration of time spent in the i_{th} 100ft deviation interval, the probability of vertical overlap can be estimated by $P_z(|1000 - D_i|)$, where D_i is the magnitude of deviation of the i_{th} interval. As in the case with a deviation between S_z and $2S_z$, the absolute value is required because for the time spent in deviation greater than 1000ft, the aircraft is at a separation of D_i-1000 from aircraft on FL_1. However, it is again also true that for the time spent in deviation greater than 1000ft, the aircraft is at a separation of 2000-D_i, from aircraft on FL_2 and, in this case, for the time spent in deviation greater than 2000ft the aircraft is at a separation of 3000-D_i from aircraft on FL_3. To account for this, the time spent in the intervals greater than 1000ft are again added in to

the corresponding intervals between FL_0 and FL_1. Thus, in the modelling, the risk at e.g. a deviation of 2400ft, which is a separation of 400ft from aircraft on FL_2 and 600ft from aircraft on FL3 is approximated by adding the times t_{14} and t_{24} as if they were separate deviations of 400 and 1400ft deviation from aircraft at FL_1.

If $S_i = |1000 - D_i|$, then the expression for $P_z(S_i)$ can again be estimated using Equation 41.

Although for deviations greater than $1.5*S_z$ it would be possible to work out the time spent in the 100ft intervals greater than $1.5*S_z$, in practice this is not necessary since $P_z(S_z\text{-}D_i)$ is sufficiently smaller in value than $P_z(2S_z\text{-}D_i)$. Deriving the times per 100ft intervals is therefore limited to the range up to $1.5*S_z$.

4.3.1.2.- Modelling the combined effect of atypical altitude deviations involving aircraft in climbing/descending flight, for S_z=1000ft

The time histories of all the large height deviations involving climbing/descending flight can be used to build a modified distribution of AAD per 100ft intervals up to $1.5*S_z$. The distribution is modified in that the time spent in deviation greater than S_z has been added into the appropriate time intervals as described in Case 2 and Case 3 above.

The probability of vertical overlap, for atypical height deviations, is then expressed by the following formula:

$$P_z(S_z) \approx \sum_i \frac{t_{AAD\,i}}{T} \times 2\lambda_z \int_{-\infty}^{\infty} f^{TVE}(z)\, f^{TVE}(z - |S_z - AAD_i|)\, dz$$

Equation 56

where t_{AADi} denotes the total time spent by aircraft with a deviation of magnitude D_i and T is the amount of flying time.

The risk is given by Equation 31, with the appropriate vertical relative speed for climbing/descending traffic and the probability of vertical overlap, $P_z(S_z)$, obtained using Equation 56.

For the case where the AAD is 1000ft, the probability of vertical overlap for aircraft nominally at the same flight level, $P_z(0)$ is calculated from the density of TVE defined in 4.2.5.3 as:

$$P_z(0) = \frac{2\lambda_z}{v_z}$$

Equation 57

4.3.1.3.- Modelling the combined effect of atypical altitude deviations by aircraft in level flight, for S_z=1000ft

The time histories of all the large height deviations involving aircraft in level flight can be used to build a similar modified distribution of AAD per 100-ft intervals up to 1.5*S_z. The distribution is again modified in that the time spent in deviation greater than S_z has been added in to the appropriate time intervals as described in Case 2 and Case 3 above.

The probability of vertical overlap is expressed by the same formula as in 4.3.1.2 and the collision risk is given by Equation 31, with the appropriate vertical relative speed for level flight traffic and the probability of vertical overlap, $P_z(S_z)$, obtained using Equation 56.

For the case where the AAD is 1000ft, the probability of vertical overlap for aircraft nominally at the same flight level, $P_z(0)$ is calculated from the TVE defined in 4.2.5.3:

$$P_z(0) = \int_{-\lambda z}^{\lambda z} \int_{-\infty}^{\infty} f_1^{TVE}(z_1) f_2^{TVE}(z_1 - z) dz_1 dz$$

Equation 58

An approximate value is given by:

$$P_z(0) = 2\lambda_z \int_{-\infty}^{\infty} f_1^{TVE}(z_1) f_2^{TVE}(z_1) dz_1$$

Equation 59

4.3.2.- Total vertical collision risk

The total vertical risk is the sum of the technical risk and the risks due to large height deviations involving both climbing/descending aircraft and level flight aircraft. As it has been said, it is assumed that the same type of collision risk model applies to the different risk components, being only different the probability of vertical overlap, $P_z(S_z)$, and the average relative vertical velocity used in each case. So,

$$N_{az(total)} = N_{az(tech)} + N_{az(climb/descend)} + N_{az(level)}$$

Equation 60

No data related to large height deviations in the EUR/SAM Corridor have been provided for this study. It is therefore impossible to quantify the value of $P_z(S_z)$ to be used in the models described above.

Data from others airspaces have been queried in order to find information about large height deviations. In [Ref. 12], the operational risk has been calculated for the EUR airspace using 90 reports on large height deviations. 65 reports out of 90 corresponded to errors caused either by the pilot, the controller or a pilot-controller loop error.
Although the probability of having large height deviations caused by contingency events (such as engine fault, pressurization failure, etc) or those caused by TCAS and their magnitude can be assumed to be the same in all airspaces, large height

deviations due to operational errors (pilot or controller errors) may be quite different depending on the type of airspace.

As the continental EUR airspace differs widely from the EUR/SAM oceanic airspace and, as it has been said, operational errors in the EUR airspace are about 75% of the total number of large errors, it is considered that it is not appropriate to use data from the EUR airspace to estimate the overall risk in the EUR/SAM Corridor.

Thus, until data on large height deviations corresponding to the EUR/SAM Corridor are reported, the overall collision risk cannot be assessed without the risk of it being underestimated.

5.- CONCLUSIONS

The collision risk assessments in this report are considerably hindered by a lack of data. Specially, a fairly large sample of data describing lateral and vertical deviations, particularly on the larger and more infrequent deviations, is needed to be able to model confidently the probability density function of the lateral and vertical deviations used to obtain overlap probabilities. Since these data were not available for this report, some conservative assumptions had to be made.

Taking this into account, the following conclusions can be extracted from the analysis of the different parameters of the collision risk models:

- Lateral collision risk assessment.

  - The probability of lateral overlap increases as the separation between routes decreases, as it was expected. The value obtained for $S_y = 50\text{NM}$ is

$P_y(50) = 8.645 \times 10^{-8}$, whilst the lateral overlap probability obtained for $S_y = 90\text{NM}$ is $P_y(50) = 2.891 \times 10^{-8}$.

- For current traffic levels, the lateral collision risk obtained is 1.62×10^{-9}, whilst the lateral collision risk estimated for 2015 with an annual traffic growth rate of 4% is 2.40×10^{-9}, and 3.19×10^{-9} if the annual traffic growth rate is of 7%. These values do not take into account traffic on the RANDOM route. However, as traffic on this route only represents 5% of the traffic in the Corridor, it is considered that the collision risk due to this route will not make the collision risk go above the TLS and the system is considered to be laterally safe until 2015.

- Vertical risk assessment.

  - Vertical risk is split into two parts, one for the technical vertical risk and the second one for the vertical risk due to all causes. The same collision risk model is used for both. The differences are the value of the vertical overlap probability and the relative vertical speed to use in each one.

  - The probability of vertical overlap due to technical causes was based on the probability distribution of Total Vertical Error (TVE). This was obtained by convoluting probability distributions of Altimetry System Errors (ASE) and typical Assigned Altitude Deviation (AAD). In the absence of any direct monitoring data from the EUR/SAM Corridor, height-keeping data and models from the EUR airspace have been used. These data were also being reviewed when this assessment was made. So, it would be recommended to repeat this study when definitive data from the EUR report are available.

  - The value of the vertical overlap probability obtained for S_z=1000ft is $P_z(1000) = 1.5447 \times 10^{-9}$. A more conservative value, used in the NAT has also been considered, i.e. $P_z(1000) = 2.46 \times 10^{-8}$.

- The vertical overlap probability obtained, $P_z(1000) = 1.5447 \times 10^{-9}$, meets the global system specification that requires the probability of vertical overlap not to exceed a value of 1.7×10^{-8}.

- The global height-keeping performance specification also specifies bounds for the proportions of height-keeping deviations larger in magnitude than 300ft, 500ft, 650ft and between 950 and 1050ft. The results show that the first and the fourth critera are met, being the remaining criteria only slightly exceeded.

- As no data on crossing traffic were available for this report, the occupancy value for crossing traffic used in the study made by ARINC, projected to the current time using an annual traffic growth rate of 5.4% has been used in this case. This estimation should be reviewed when data from other FIR/UIRs are available.

- As far as the technical vertical risk is concerned, the value of the collision risk for the current traffic levels is estimated to be 8.01×10^{-11} or 1.28×10^{-9}, depending on the vertical overlap probability used (the first value corresponds to the calculated $P_z(1000)$ and the second one, to the conservative value used in the NAT). The technical vertical collision risk estimated for 2015 with an annual traffic growth rate of 4% is 1.19×10^{-10} for the calculated vertical overlap probability and 1.89×10^{-9} for the NAT probability. If the annual traffic growth rate is of 7% the technical risk is 1.58×10^{-10} and 2.51×10^{-9}, depending again on the vertical overlap probability used. These values are under the TLS for technical vertical risk, 2.5×10^{-9}, even in 2015 and with an extremely conservative vertical overlap probability.

- It has not been possible to obtain the overall vertical risk, since no large height deviation reports were available from the EUR/SAM Corridor. Data from the

EUR airspace was available, but as the continental EUR airspace differs widely from the EUR/SAM oceanic airspace and operational errors (large deviations due to pilot-controller loop errors) in the EUR airspace are about 75% of the total number of large errors, it is considered that it is not appropriate to use data from the EUR airspace to estimate the overall risk in the EUR/SAM Corridor.

As the accuracy of the assessment greatly depends on the availability and accuracy of the data provided, it is recommended that:

- accurate flight progress data be made available from all FIR/UIRs to facilitate the verification of traffic flows, distribution and passing frequencies used in the analysis, cross-checking data obtained from Picasso;

- the crossing traffic occupancy be recomputed when data for all crossing routes becomes available;

- data on lateral and vertical deviations obtained from radar data and incident reports be provided in order to improve the estimation of overlap probabilities;

- this assessment be reviewed and updated when definitive data on ASE distributions in the EUR airspace are available.

6.- ACRONYMS

AAD	ASSIGNED ALTITUDE DEVIATION
ADS	AUTOMATIC DEPENDENT SURVEILLANCE
ASE	ALTIMETRY SYSTEM ERROR
ATC	AIR TRAFFIC CONTROL
ATS	AIR TRAFFIC SERVICES
EUR/SAM	EUROPE/SOUTH AMERICA
FIR	FLIGHT INFORMATION REGION

FL	FLIGHT LEVEL
FMC	FLIGHT MANAGEMENT COMPUTER
FTE	FLIGHT TECHNICAL ERROR
HFDL	HIGH FREQUENCY DATA LINK
HMU	HEIGHT MONITORING UNIT
kts	KNOTS
MASPS	MINIMUM AVIATION SYSTEM PERFORMANCE STANDARDS
MDG	MATHEMATICS DRAFTING GROUP (EUROCONTROL)
NAT	NORTH ATLANTIC
NM	NAUTICAL MILE
RGCSP	REVIEW OF THE GENERAL CONCEPT OF SEPARATION PANEL
RNP	REQUIRED NAVIGATION PERFORMANCE
RVSM	REDUCED VERTICAL SEPARATION MINIMUM
SAT	SOUTH ATLANTIC
SATCOM	SATELLITE COMMUNICATIONS
SATMA	SOUTH ATLANTIC MONITORING AGENCY
STATFOR	AIR TRAFFIC STATISTICS AND FORECASTS (EUROCONTROL)
TVE	TOTAL VERTICAL ERROR
UIR	UPPER FLIGHT INFORMATION REGION

7.- REFERENCES

[Ref. 1] Atlas South Atlantic Crossing 57C, 04 Oct 01. Carta de Navegación Aérea.

[Ref. 2] Risk Assessment of RNP10 and RVSM in the South Atlantic Flight Identification Regions Including an Assessment for Limited Implementation of RVSM on RN741. (ARINC)

[Ref. 3] Comparativa ARINC-CRM para tres rutas

[Ref. 4] AIP Spain. AIS. AIC 17/Jan/01

[Ref. 5] Separation and Airspace Safety Panel. A New Parameter for Gross Lateral Errors (SASP-WG/A/2-WP/4, 21/10/01)

[Ref. 6] Separation and Airspace Safety Panel. Proposed Guidance of Specifying Performance Requirements for Automatic Dependent Surveillance (SASP-WG/A/2-WP/10 22/10/01)

[Ref. 7] Manual on airspace planning methodology for the determination of separation minima (ICAO Doc 9689-AN/953)

[Ref. 8] ADS Europe Complementary Analysis Studies. Performance measurement on ADS/ATN and ADS/FANS1 systems

[Ref. 9] Air Traffic Services Planning manual. Doc 9426 OACI

[Ref. 10] Estudio ASIN. Situación del tráfico del pasillo EUR/SAM en el FIR/UIR Canarias. 13/05/5

[Ref. 11] ICAO Document 9574 (2nd edition). Manual on Implementation of a 300m (1000ft) Vertical Separation Minimum between FL290 and FL410 inclusive.

[Ref. 12] RVSM report 2005.- MDG/32 DP/07. 32nd Meeting, 28th to 30th September 2005

[Ref. 13] RVSM Safety Assessment of the Australian Airspace for the period 1 Jan 2004 through 31 Dec 2004.- RASMAG/3-WP/16 06/06/2005. OACI

[Ref. 14] Summary of the Airspace Safety Reiew for the RVSM Implementation in Asia Region.- RASMAG/4-WP11 25/10/2005. OACI

[Ref. 15] The EUR RVSM Mathematical Supplement.-MDG/21 DP/01 August 2001.

ANNEX 1

METHODS FOR OCCUPANCY ESTIMATE

A1.1.- DEFINITION

The concept of same direction lateral occupancy for a parallel tracks system refers to the average number of aircrat which are, in relation to the typical aircraft:

- flying in the same direction as it
- nominally flying on tracks one lateral separation standard away from it
- nominally at the same flight level as it; and
- within a longitudinal segment centered on it.

The above definition has been expanded to include tracks that are separated by more than one lateral separation standard because there is a significant collision risk arising from the probability of overlap between non adjacent tracks.

A similar set of criteria can be used to define opposite direction occupancy, just replacing "flying in the same direction as it" by "flying in the opposite direction".

The length of the longitudinal segment, $2S_x$, is considered to be the length equivalent to 20 minutes of flight at 480kts.

A1.2.- METHODS FOR OCCUPANCY ESTIMATE

There are two methods to estimate lateral occupancy, called "Steady state flow model" and "Direct estimation from time at waypoint crossing".

The first one is the only way of achieving an estimation of the occupancy when only records of daily traffic are available or if, in the direct estimation from time at waypoint crossing there are not big amounts of hourly information. The method of direct estimation provides more precise estimations and it is, generally, preferred.

For a given system, lateral occupancy, E_y, can be expressed as:

$$E_y = \frac{2T_y}{H}$$

Equation 61

Where:

- T_y represents the proximity time generated in the system, i.e. the total time spent by aircraft pairs on adjacent flight paths at the same flight level and within a longitudinal distance S_x of each other.

- H represents the total number of flight hours generated in the system during the considered period of time.

A1.2.1.- STEADY STATE FLOW MODEL

This section is a transcription of sections 2.3, 3.1, 3.2 y 3.3 and appendix C of Chapter 4, Section 2, part II of [Ref. 9].

The occupancy E_y will be estimated for a parallel routes system in which it will be supposed that the flow of traffic towards the flight paths and along them is statistically stable during the considered period.

For a general system, the occupancy will be obatined as a weighted sum of the occupancy of all the subsystems "in stable state", with respect to the number of flight hours generated in each one.

Tracks are numerated from 1 to t and flight levels from 1 to f. The traffic flow on track i, at flight level j (flight path ij) is m_{ij}, i.e. m_{ij} aircraft cross every point of the track every hour. The length of the track is L and it is assumed that all aircraft fly at the same speed V. T is the time during wich the system is observed.

A1.2.1.1.- Number of flight hours H

The time L/V is needed for an aircraft to fly through the system. So, in the flight path ij there are always $m_{ij} \cdot L/V$ aircraft and the number of aircraft in the whole system will be:

$$\sum_{i=1}^{i=t} \sum_{j=1}^{j=f} m_{ij} \cdot \frac{L}{V}$$

Equation 62

From this equation it is deduced that:

$$H = \frac{T \cdot L}{V} \sum_{\text{all trajectories ij}} m_{ij}$$

Equation 63

A1.2.1.2.- Total proximity time T_y

Calculation of T_y is a little bit more complicated. Let's consider an aircraft on the flight trajectory ij: the foreseen number of proximate aircraft on the adjacent flight trajectory i-1 is given by:

$$\frac{2 \cdot S_x}{V} \cdot m_{i-1,j}$$

Equation 64

So, during the L/V flight hours of this aircraft, the proximity time generated is:

$$\frac{2 \cdot S_x}{V} \cdot m_{i-1,j} \cdot \frac{L}{V}$$

Equation 65

During the T hours in which the system is observed, m_{ij}*T aircraft fly on the flight path ij, and the proximity time generated between trajectory ij and trajectory i-1,j is:

$$\frac{2 \cdot S_x}{V} \cdot m_{i-1,j} \cdot \frac{L}{V} \cdot m_{ij} \cdot T$$

Equation 66

The total proximity time, T_y, is obtained adding all the previous pairs:

$$T_y = \sum_{i=1}^{i=t} \sum_{j=1}^{j=f} \frac{2 \cdot S_x}{V} m_{i-1,j} \cdot \frac{L}{V} \cdot m_{i,j} \cdot T$$

Equation 67

Or (simplifying notation):

$$T_y = \sum_{\substack{\text{all pairs} \\ \text{of tracks}}} m_{i-1,j} m_{i,j} \cdot \frac{2 \cdot S_x \cdot L \cdot T}{V^2}$$

Equation 68

A1.2.1.3. Occupancy

Substituting Equation 63 and Equation 68 into Equation 61, occupancy is finally given by:

$$E_y = \frac{2 \cdot T_y}{H} = \frac{2 \cdot \sum_{\substack{\text{all pairs} \\ \text{of tracks}}} m_{i-1,j} m_{i,j} \cdot \frac{2 \cdot S_x}{V}}{\sum m_{i,j}}$$

Equation 69

For same direction lateral overlap, aircraft flying on adjacent tracks in the same direction and at the same flight level must be considered. For opposite direction lateral overlap, aircraft flying on adjacent tracks in the opposite direction and at the same flight level must be considered.

If the system is not statistically stable, as it happens in the case in which traffic flows depend on the time, the occupancy value E_y should be calculated adding all the subsystems that are in a stable state. Thus, if there are r subsystems of this type:

$$E_y = \frac{2\sum_{p=i}^{p=r} T_y{}^p}{\sum_{p=i}^{p=r} H^p} = \frac{\sum_{p=i}^{p=r} H^p E_y{}^p}{\sum_{p=i}^{p=r} H^p}$$

Equation 70

Where the subindex p indicates that the value corresponds to the subsystem p. T_J^p and H^p can be obtained for every subsystem p using the method described before.

A1.2.2.- DIRECT ESTIMATION FROM TIME AT WAYPOINT PASSING

This has been the method used in this report.

It is based on the dayly flight progress data of aircraft in the tracks system studied. The period of time of available flight progress data should be long enough, in order to be able to detect any importat variation in the traffic flow.

Basically the method consists in examining the crossing time notified by all the aircraft of the system at a given waypoint.

The points utilized as reporting points must be approximately on a plane at right angles to the track system, in order to be able to compare passing times of aircraft on one route with passing times of aircraft on another route. That is why, in this study, the selected points as

points for time passing comparison were the south fixes of each route (EDUMO, TENPA, IPERA y GUNET).

This comparison will give the number of proximate pairs. A proximate pair, between aircraft on adjacent routes and at the same flight level, is defined as the occurrence of two aircraft passing within a given longitudinal distance $2S_x$. If both aircraft fly in the same direction it will be a proximate pair in the same direction, whilst it will be an opposite direction proximate pair if they fly in opposite directions. As far as the distance S_x is concerned, it is often given by the time T_0, being the time it takes an aircraft with an average speed of 480kts to fly that distance. In this study, S_x is 80NM and T_0, 10 minutes.

If, for each and every flight level, passing times at the reporting point of all aircraft on one route are compared with the passing times of all aircraft on another route at the homologous reporting point, the number of proximate pairs between these two routes will be given by the number of cases in which the absolute vaue of the difference between both times is less than 10 minutes.

The same procedure must be followed with the remaining pairs of routes.

Considering all this, occupancy can be estimated using the following equation:

$$E_y = \frac{2n_y}{n}$$

Equation 71

where n_y is the total number of proximate pairs of aircraft and n is the total number of aircraft in the system.